Project acronym and title:
SECURe – Subsurface Evaluation of Carbon capture and storage and Unconventional risks

D5.4 GUIDELINE ON RANKING OF VARIOUS SQUEEZE SEALANT MATERIALS WITH RESPECT TO EASE OF PLACEMENT

Authors and affiliation:
Laura Edvardsen, Jelena Todorovic, Ali Taghipour, Amir Ghaderi, Mohammad Hossain Bhuiyan, Pierre Cerasi

SINTEF Industry, Department of Petroleum, S. P. Andersens vei 15B, 7031 Trondheim, Norway

Email of lead author:
laura.edvardsen@sintef.no

D5.4
Revision:1

Project funded by the European Commission within the Horizon 2020 Programme		
Dissemination Level		
PU	*Public*	*X*

Deliverable number:	**5.4**
Deliverable name:	**GUIDELINE ON RANKING OF VARIOUS SQUEEZE SEALANT MATERIALS WITH RESPECT TO EASE OF PLACEMENT**
Work package:	**WP5 Impact Mitigation and Remediation**
Lead WP/deliverable beneficiary:	SINTEF Industry

Status of deliverable		
	By	**Date**
Submitted (Author(s))	**Laura Edvardsen, Ali Taghipour, Amir Ghaderi, Mohammad Hossain Bhuiyan, Jelena Todorovic, Pierre Cerasi**	**30.10.2020**
Verified (WP leader)	**Pierre Cerasi**	
Approved (EB member)	**Jens Wollenweber**	
Approved (Coordinator)	Edward Hough	06.11.2020

Author(s)		
Name	**Organisation**	**E-mail**
Laura Edvardsen	**SINTEF**	**Laura.edvardsen@sintef.no**
Jelena Todorovic	**SINTEF**	**Jelena.todorovic@sintef.no**
Ali Taghipour	**SINTEF**	**Ali.taghipour@sintef.no**
Amir Ghaderi	**SINTEF**	**Amir.ghaderi@sintef.no**
Mohammad Bhuiyan	**SINTEF**	**Mohammad.bhuiyan@sintef.no**
Pierre Cerasi	**SINTEF**	**Pierre.cerasi@sintef.no**

Public introduction

Subsurface Evaluation of CCS and Unconventional Risks (SECURe) is gathering unbiased, impartial scientific evidence for risk mitigation and monitoring for environmental protection to underpin subsurface geoenergy development. The main outputs of SECURe comprise recommendations for best practice for unconventional hydrocarbon production and geological CO2 storage. The project is funded from June 2018–May 2021.

The project is developing monitoring and mitigation strategies for the full geoenergy project lifecycle; by assessing plausible hazards and monitoring associated environmental risks. This is achieved through a program of experimental research and advanced technology development that includes demonstration at commercial and research facilities to formulate best practice. We will meet stakeholder needs; from the design of monitoring and mitigation strategies relevant to operators and regulators, to developing communication strategies to provide a greater level of understanding of the potential impacts.

The SECURe partnership comprises major research and commercial organisations from countries that host shale gas and CCS industries at different stages of operation (from permitted to closed). We are forming a durable international partnership with non-European groups; providing international access to study sites, creating links between projects and increasing our collective capability through exchange of scientific staff.

Executive report summary

This report details the experimental campaign at SINTEF to test remediation fluids, in order to quickly mitigate leakage from subsurface injection or production from a well. A three-tiered experimental methodology is developed, whereby the candidate remediation chemistry is first tested in a rectangular slit in a cement plug, then in a similar set-up but where a stress-induced fracture replaces the slit, and finally in SINTEF's new ECCSEL Well Integrity research infrastructure, a CT-transparent mini-wellbore simulator. Due to Covid-19 and delays in developing new remediation materials in WP5, the following materials were tested: silica gel, Portland low-density cement and Portland flexible cement. The report shows that the different tiers make for a good methodology to assess strengths and weaknesses of the tested materials, with respect to placement, type of fracture to be remediated and geomaterials in presence. At this stage of development, it was not possible to test all materials in all three tiers of testing: however, it would seem that flexible cement ranks higher than low-density cement, itself preferable to silica gel.

Contents

FIGURES

TABLES

1 Introduction

1.1 THE AIM OF THIS WORK

The aim of work was to test the sealing ability of different sealants for leakage pathways in the cement sheath. The remediation method used in this study is squeeze cementing. The technique was simplified compared to the typical way it is performed in the field, by avoiding a need to perforate the casing. The squeeze cementing experiments were performed in the newly acquired equipment from the Well Integrity ECCSEL Research Infrastructure. In order to create a realistic case of cement sheath failure, a specially designed pressure cell that allows application of both confining pressure, pore pressure and casing pressure on downscaled wellbore samples (including casing, cement and rock) was used in this work. The pressure is applied from within the casing to fracture the cement first, and then sealant material is injected into the annulus through an inlet on the top or bottom side of the cell. Another advantage of this setup is that the entire experiment can be monitored in-situ in a CT scanner. Permeability of the cement sheath is measured before and after sealant injection.

Several sealing materials were tested in this study:

1. Ordinary Portland G cement (reference sealant)
2. Flexible Portland G cement (formulated in-house)
3. Silicate gel (formulated in-house)

The aim of our laboratory tests is to determine how suitable are these selected materials for remediation of CO_2 leakage through a fractured cement sheath. The outcome of this task was originally planned to be a ranking of various sealant materials for squeeze cementing with respect to easy of placement and sealing performance. Therefore, other novel sealing materials were considered in the planning stage, but this was not accomplished due to delays caused by the COVID-19 pandemic. Further activities will build on this study and consider how it could be expanded to include the unconventional hydrocarbon industry.

1.2 SQUEEZE CEMENTING

Squeeze cementing is the most common remediation method in the O&G industry for cement sheath that failed to maintain zonal isolation. Squeeze cementing encompasses different methods of pumping cement slurry or some other sealing material through perforations in the casing/liner to remediate failure of the cement in the annulus, or to fill holes or fissures in the casing/liner itself. There are other applications of this method such as sealing lost circulation zones and zonal isolation. Squeeze cementing is usually performed during well completion (when the casing is run into the well), but it can be used later on in the lifetime of the well as a remediation method. Squeeze cementing techniques have been thoroughly covered in the following references (Nelson & Guillot, 2006; Manceau et al., 2014; Todorovic et al., 2016a). Examples of different squeeze cementing techniques and possible applications are listed in Table 1.

Table 1 Examples of squeeze cementing techniques and possible applications, adopted from (Todorovic et al., 2016a).

Squeeze cementing technique	Possible applications
Low- pressure squeeze (i.e. pumping pressure below the formation fracturing pressure)	Failure of cement or casing/liner in the production zone
Circulating squeeze at low pressure with cement retainer or packer	Cement failure; casing or liner leak
High-pressure squeeze (i.e. pumping pressure above the formation fracturing pressure)	Cement failure (mud channels, cracks, micro-annuli, repairing casing shoe or cement at the top of the liner)
Block squeeze at high pressure with cement retainer or packer	Zonal isolation of a permeable zone – a preventive measure
Bradenhead squeeze with coiled-tubing and retainer or packer; hesitation pumping	Cement failure; casing or liner leak; cementing casing shoe; loss of circulation during drilling

To the best of our knowledge, squeeze cementing method has been used previously in only a few laboratory studies with the purpose of testing efficacy of different sealing materials for remediation of leakage through cement sheath (Todorovic et al., 2016b; Ho et al., 2016; Tavassoli et al., 2018; Abdulfarraj and Imqam, 2020). Injection of reactive fluids or sealing materials in a core flooding setup is a standard method of testing efficacy of different interventions in reservoir engineering, and this method was also used to simulate squeeze cementing technique into cement cores with leakage paths. In our previous study, a standard core flooding setup was used to remediate artificially created leakage pathways in a cement core by injecting a thermally activated sealant and allowing it to cure at a designated temperature (Todorovic et al., 2016b). Permeability was measured prior to and after sealant injection. The leakage pathways (vertical rectangular channels) were created during cement setting by using a plastic mould for channels and a rubber sleeve to shape the core. Simple leakage pathways can be also created by sawing cement cores in half and placing them against each other or another material, or by fracturing cement cores using the Brazilian method (Ho et al., 2016; Tavassoli et al., 2018). A pH-activated polymer gel was then used to seal the fractures in these two studies (Ho et al., 2016; Tavassoli et al., 2018), and the efficacy of the treatment was tested by injecting water, acidic brine and gas-CO_2 after the polymer had set. A similar study of remediation of a designed leakage path through cement core using micro-sized crosslinked polymer gel was recently reported (Abdulfarraj and Imqam, 2020). Leakage pathway was created by inserting two metal sheets between two halves of a cement core that were cured on their own in a cylindrical mould cut in half. Water breakthrough measurements were performed after gel placement, like in (Ho et al., 2016; Tavassoli et al., 2018), to measure the gel strength and sealing efficacy. The artificial "fractures" created in-situ during cement curing or simply by dividing a cement core in some manner and inserting some kind of spacer, are fundamentally different from fractures that arise from thermal or pressure cycling of the casing (De Andrade et al., 2016; Skorpa et al., 2019; Vrålstad et al., 2019).

It is worth noting that similar studies of sealant injection into fractured or porous rock samples have been much more frequently reported than for cement (Tongwa et al., 2013; Li et al., 2014; Syed et al., 2014; Durucan et al., 2016; Mosleh et al., 2016; Fleury et al., 2017). For example, Tongwa et al. (2013) tested performance of four potential sealants (paraffin wax, polymer-based gel, silica-based gel, and micro-cement) on reservoir and caprock samples that had an artificial rectangular fracture along the length. The shape of the "fracture" in the rock cores (Tongwa et al., 2013) was similar to the artificial fractures created in the cement cores in the study by Abdulfarraj and Imqam (2020).

We used squeeze cementing method in this work to study behaviour of different alternative sealing materials in downscaled wellbore model samples. The squeeze technique was modified to comply with the needs of our equipment but without compromising with the efficacy of the method. In order to avoid the need for casing perforation and to simplify the design of the equipment, the sealant fluids were injected axially in our study. The experimental setup with the pressure cell (mini-wellbore simulator) used in this work were much more sophisticated than a standard core flooding setup, and it recreates downhole conditions more realistically. The most important feature is that realistic fractures are created in the cement sheath by pressurizing the casing from the inside. Pressure-induced fractures in the cement, although providing a more realistic indication of efficacy of remediation, are unique for each wellbore-model sample, which means that different tests and sealants cannot be directly compared. Therefore, a standard core flooding setup was also used for the trial tests on cement cores with artificial "fractures" (i.e. flow pathways created in a controlled manner). Moreover, this was necessary especially for the sealants that the previously have not been tested in the mini-wellbore simulator, in order to understand better their behaviour during injection and curing and to optimize the injection procedure for the mini-wellbore simulator.

1.3 ALTERNATIVE SEALING MATERIALS

There are many novel materials and commercially available products that have potential to replace standard wellbore cement for certain applications, such as remediation of leakage caused by failure of the cement in the annulus. Some of the requirements for materials that could replace cement are long-term durability, no shrinkage, negligible permeability (also for gas), non-brittleness, deformability and chemical stability (Abdollahi et al., 2016). Sealing materials that could be alternatives to cement for a squeeze cementing operation are summarized in Table 2, including their other potential applications. There are alternative sealing materials that could be used for different well cementing applications, including leakage prevention and cement repair. Some examples are cements with a latex-based component (Pike, 1997; Sun et al., 2006; Mosleh et al., 2017), geopolymers (Davidovits, 2015; Khalifeh et al., 2016, 2017, 2018; Salehi et al., 2016), blast furnace slag (BFS) (Saasen et al., 1994; Cowan et al., 1992; Daulton et al., 1995), and low melting point metal alloys (Carpenter et al., 2004). Some of these sealant materials are well-known in the O&G industry, whereas others have been developed relatively recently and are the focus of current research and development.

Table 2 Overview of alternative sealing materials that have a potential to be used for squeeze cementing (e.g. remediation of leakage caused by failure of the cement in the annulus). Adapted from SECURe Deliverable 5.1 and extended.

Sealing material	How it works?	Potential applications
Polymer-based gels	Most polymer-gel systems are based on cross-linking of polymers with a heavy metal ion in a brine or water solution. Polyacrylamide is mainly used by the industry. Chromium III is the most commonly used cross-linker, but boron, aluminium and zirconium could be more environmentally friendly alternatives.	• Cement failure and formation failure in near well region (Tongwa et al., 2013; Li et al., 2014; Syed et al., 2014; Ho et al., 2016; Mosleh et al., 2016; Korre et al., 2017; Khanna et al., 2018; Tavassoli et al., 2018, 2019; Abdulfarraj and Imqam, 2020) • Injection of polymer-gels is a common practice in the O&G industry for enhanced oil recovery and reservoir treatment.
Thermosetting polymers (resins)	Resins are particle-free fluids that are designed to solidify into an impermeable material at a predefined temperature according to the downhole conditions in question.	• Repair of cement failure by squeeze operation (Al-Ansari et al., 2015; Todorovic et al., 2016b) • Repair of casing leaks (Sanabria et al., 2016) • Lost circulation material (Knudsen et al., 2014) • P&A (Beharie et al., 2015; Davis, 2017)
Silicate-based gels	Silicate-based solutions are very reactive and form amorphous silica in the presence of CO_2. The complex process of precipitation is described elsewhere (Fleury et al., 2016, 2017; Castaneda-Herrera et al., 2018).	• Repair of cement failure by squeeze operation • Formation failure in the near well region (Lakatos et al., 2009, 2012a, 2012b, 2020; Tongwa et al., 2013; Karas et al., 2016; Fleury et al., 2017; Wiese et al., 2019)
Geopolymers	Geopolymers are alkali-activated binders that are prepared by mixing an aluminosilicate source material such as fly ash, kaolin, metakaolin, and BFS, with an activator (e.g. alkaline solution NaOH, KOH, and LiOH; and/or an alkaline silicate solution Na_2SiO_3, K_2SiO_3) (Sukmak et al., 2013; Zuhua et al., 2009; Autef et al., 2013; Özodabaş et al., 2013). Depolymerization, transportation or orientation of oligomers, and polycondensation are the three main mechanisms in the formation of geopolymers (Davidovits, 2015).	• Well cementing applications (Khalifeh et al., 2016, 2017, 2018; Salehi et al., 2016) • Not tested yet as remediation material

Use of foams, polymer-based gels and inorganic gels is common practice in the O&G industry for mitigating different issues that may arise during production (Tongwa et al., 2013; Manceau et al., 2014; Syed et al., 2014; Wessel-Berg et al., 2015; Durucan et al., 2016; Mosleh et al., 2016; Korre et al., 2017; Lakatos et al., 2009, 2012a, 2012b; Fleury et al., 2016, 2017; Karas et al., 2016; Castaneda-Herrera et al., 2018; Wiese et al., 2019; Abdulfarraj and Imqam, 2020). Loss of conformance within the reservoir can be mitigated by CO_2 mobility control and flow diversion. For example, injection of a cross-linked hydrolysed polymer-gel is typically used in the O&G industry for enhanced oil recovery, to improve conformity of fluid flow in the reservoir and for remediation of leakage in the near-well region (Seright 2009; Zhang and Bai 2010; Yu et al. 2017; Imqam et

al. 2015a, b, 2018). Inorganic silicate gels are a proven remediation product which has the ability to reduce the permeability of rock formation. Silicate gels have a potential for deep penetration into the rock, good thermal and chemical stability, environmental friendliness and low cost (Castaneda-Herrera et al., 2018; Wiese et al., 2019; Lakatos et al., 2020). Silicate gels can be engineered to respond to the presence of CO_2 in order to control leakage (Brydie et al., 2014; Fleury et al., 2017; Castaneda-Herrera et al., 2018; Wiese et al., 2019). The implementation of silicate gels needs testing in the acidic environment (e.g. in presence of carbonated brine).

An excellent example of field application of a silicate solution for remediation of leakage in the near-well region of the reservoir, is the case of remediation of CO_2 leakage from a collapsed well drilled into a natural CO_2 field in Bečej (Serbia) (Vrålstad et al., 2015; Karas et al., 2016). The remediation operation that was conducted in 2007, included injection of different silicate solutions (i.e. pure, with polymers and other chemicals) and cross-linker solution (Lakatos et al., 2009, 2012a; Karas et al., 2016). Another remediation operation was conducted in 2016, in the course of the MiReCOL project (Wiese et al., 2019). The laboratory studies on silicate gels, where characterization of different silicate-based solutions (gelation time, viscosity, etc.) and core flooding injection experiments were performed (Fleury et al., 2017), were preparatory work for the field tests in Bečej. However, a formulation that had no requirement for the presence of CO_2 in the reservoir to achieve gelation was especially developed for the field test (Wiese et al., 2019).

Since in practical applications, the leaking fluid may not be only CO_2, or in the case of shale gas or other subsurface energy situations, no CO_2 is already present, cost-effectiveness points to the need for any specific remediation fluid or complex procedure to mix several fluids to yield significantly better results than can be obtained with relatively low cost solutions based on variations of Portland cement, which are readily available and should "marry" better with already in place cement.

2 Experimental

2.1 SEALANT MATERIALS

To test the effect of the different sealant materials, a cement core with a prepared slit was used. The core was constructed of Portland G with a water/cement ration of 0.44. The slurry was prepared according to the API recommended practice standard (API RP 10B-2, 2013). A silicone square rod (approximately 24 mm^2) was placed in the centre of a cylindrical mould before adding the cement slurry. The cement was left to harden in room temperature and ambient pressure. After hardening, the silicone rod was removed, and the cement core was grinded before attached to a Castlegate sample using epoxy. The Castlegate acted as a filter between the cement and outlet. An overview of the sample dimensions is presented in Table 3 **Error! Reference source not found.**.

Table 3 Overview of prepared samples of Portland G core, Castlegate filter and different sealing material.

Sealing material	Portland G core		Castlegate base	
	Diameter (mm)	Length (mm)	Diameter (mm)	Length (mm)
Low-density Portland G	38.24	45.70	37.51	32.96
Flexible Portland G	38.10	50.73	37.84	37.75
Silica gel	38.22	47.85	37.93	34.39

The experimental setup is illustrated in Figure 1. Measuring the pore pressure gives an indication of sealing ability. Hence, a pore pressure test was conducted before adding the sealant materials. This was done by injecting a 5 wt% NaCl solution through the top piston, allowing the brine to escape through the bottom piston, and measure the pore pressure build up upon injection. The pore pressure was measured for different injection rates: 0.5, 1, 2, 5 and 10 mL/min, and the confining pressure was 4 MPa during all experiments.

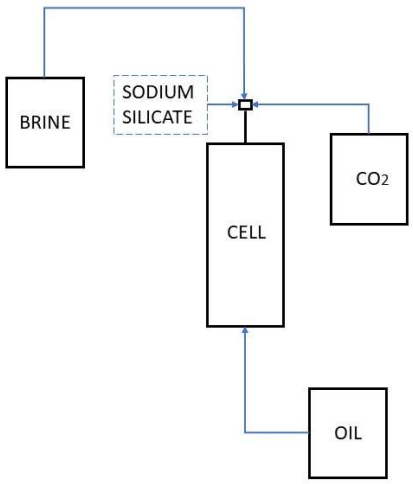

Figure 1 Illustration of the experimental setup for sealant injection into a cement core.

2.1.1 Portland G cement

Ordinary Portland G cement was selected as a reference sealant material. Portland G slurry is prepared according to the API recommended practice standard (API RP 10B-2, 2013). Slurry density is a parameter that can be varied by changing water/cement ratio and/or by introducing certain additives. A lower density slurry can be beneficial for improving the efficacy of the squeeze job, and this was selected for the injection tests. We used three formulations based on Portland G: standard Portland G (reference), low-density slurry and flexible cement (with additives).

For the low-density Portland G slurry, the water to cement ratio was set to 0.5 and the slurry was left to harden under room temperature and pressure. Figure 2 depicts the prepared slit where low-density Portland G was injected to form a sealing barrier. Excess slurry was left to harden under same the conditions and used for Unconfined Compressive Strength (UCS) tests.

Figure 2 Pictures of the prepared slit before sealant material is injected (a) and the cement- Castlegate sample (b).

Flexible Portland G cement was also tested as a sealant material. The additives used were sodium metasilicate and bentonite. Sodium metasilicate and bentonite are typically used as extending agents (Nelson & Guillot, 2006). Moreover, sodium metasilicate acts as an accelerator (Houlsby,1990; Nelson & Guillot, 2006; Cao et al., 2018). Increasing sodium metasilicate or bentonite content results in lower slurry density, but also lower compressive strength (Nelson & Guillot, 2006). Given that sodium metasilicate and bentonite will absorb some water, additional mixing water is thus needed (Nelson & Guillot, 2006), which implies water to cement ratio needs to be higher than 0.44. API/ISO recommendation for bentonite is to add 5.3 % BWOC of water for each 1 % BWOC added. Several slurries were prepared to optimize content of water and additives. After these trials, the amount of bentonite and sodium metasilicate was each set to 1 % BWOC. The water to cement ratio was set to 0.6. Dry sodium metasilicate and bentonite were first blended in the water at low speed, and then cement was added.

The slurry was injected to a cement core with a prepared slit and set to harden at room temperature and pressure. Figure 3 depicts the slit where the sealant material was injected. Excess slurry was left to harden under same the conditions and used for UCS tests.

Figure 3 Pictures of the manufactured slit before sealant material is injected (a) and the cement-Castlegate sample (b).

2.1.2 Silicate gel

The applicability of silica gel as a sealant material experiments were investigated using a cement core with a large, prepared slit. The cement-Castlegate sample was saturated with a 5 wt % NaCl solution. After saturation, the sample was placed in a cell with a confining pressure of 4 MPa. To create a silica gel barrier, 7 wt% sodium silicate solution were hardened using gaseous CO_2 were used (Castaneda-Herrera et al., 2018). Figure 4 depicts the sample before saturation.

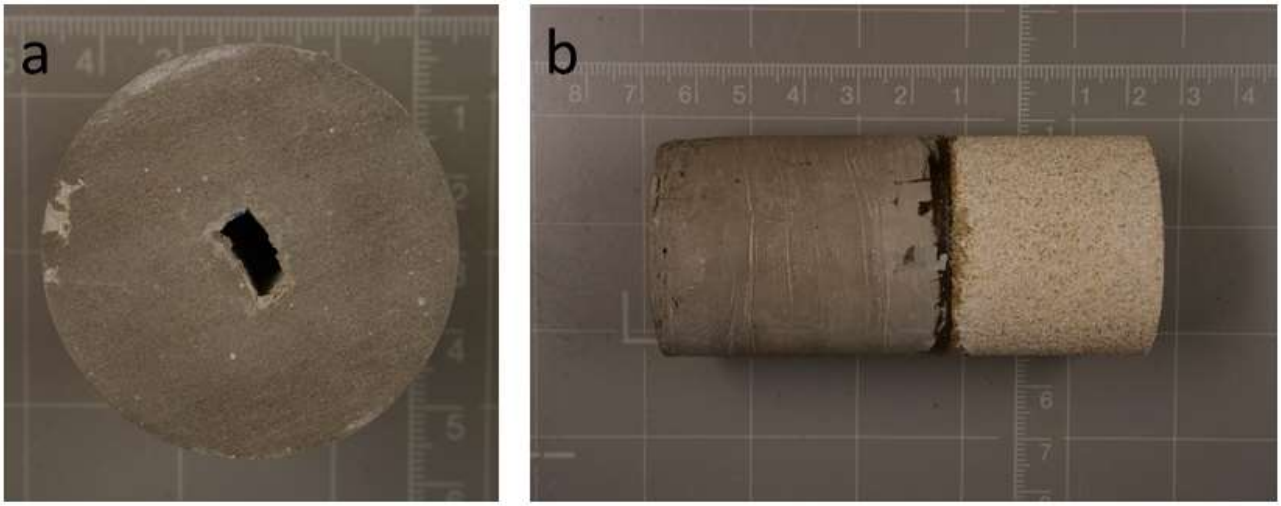

Figure 4 Pictures of the prepared slit before sealant material is injected (a) and the cement- Castlegate sample (b).

Measuring the pore pressure was done as follows in Table 4, with a confining pressure equal to 4 MPa. For all tests, the sodium silicate was added prior to CO_2 exposure.

Table 4 Description of the pore pressure test.

Test number	Description
1. Pore pressure test	A pore pressure test was conducted prior to exposure of sodium silicate and CO_2 to get a reference point.
2. Pore pressure test	Sodium silicate was poured in the induced slit. Gaseous CO_2 was injected while the outlet was open, allowing brine and CO_2 to escape the system. After 20 minutes of CO_2 injection a pore pressure test was conducted.
3. Pore pressure test	4 mL sodium silicate was injected by cell tubing through the top piston. This was followed by 1 mL brine to remove excess sodium silicate from the tubing. Gaseous CO_2 was injected while the outlet was open, allowing brine and CO_2 to escape the system. After 20 minutes of CO_2 injection a pore pressure test was conducted.
4. Pore pressure test	4 mL sodium silicate was injected by cell tubing through the top piston. This was followed by 1 mL brine to remove excess sodium silicate from the tubing. Gaseous CO_2 was injected while the outlet was open, allowing brine and CO_2 to escape the system. After 20 minutes of CO_2 injection a pore pressure test was conducted.
5. Pore pressure test	4 mL sodium silicate was injected using the cell tubing through the top piston. 1 mL brine solution was ejected from the bottom piston to remove excess sodium silicate from the tubing. The outlet was closed, and gaseous CO_2 injected for 30 minutes. After CO_2 injection, the inlet was closed, and the cell was left like this overnight. The next day, a pore pressure test was conducted.

2.1.3 Silica gel in induced fracture

A Portland G cement sample with diameter of 38.33 mm and thickness 20.70 was saturated with a 5 wt% brine solution. After saturation, a permeability test was conducted using the transient pressure equilibration method. In the direct determination experiment, a cylindrical, disk-shaped sample was mounted between two steel pistons and sintered disks, with a rubber sleeve around the cylindrical surface. The sample is exposed to a confining pressure through the sleeve and pistons (Figure 5). At the end surfaces of the sample, pore fluid may enter or escape through two sintered steel disks. The excess pore fluid is kept in two reservoirs on each side of the sample. Confining and pore pressure are applied to the sample and wait until sample is consolidated (establishment of pressure equilibrium). After consolidation, a pore pressure difference is generated across the sample by two needle valves and the ensuing evolution of the differential pressure is measured with a differential pressure transducer. The two sides of the sample are each connected to a pressure accumulator and a pump through ball valves, which give least pressure change during closing. The confining pressure is generated by a pump and an accumulator keeps the pressure constant. Pressure increase from both top and bottom was conducted (identical pressure difference) in order to increase the reliability of the measurement.

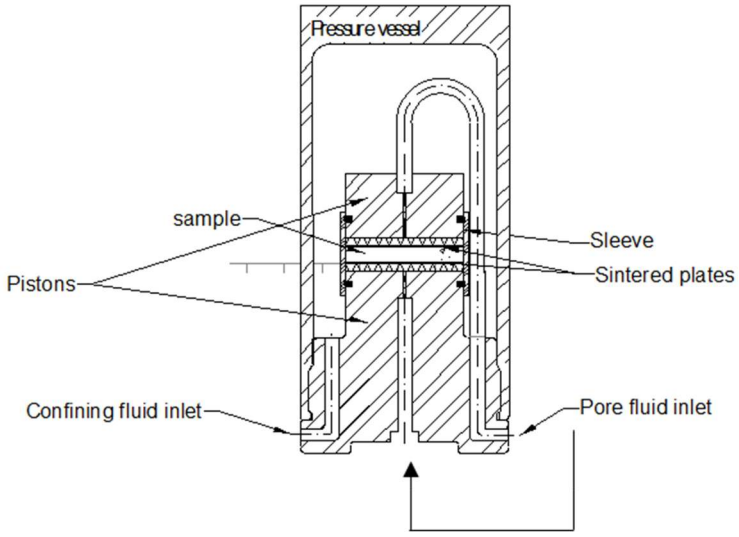

Figure 5 Schematic drawing of the cell used to measure permeability on shale thin discs under confinement.

After the permeability test, a fracture was induced to the sample using a Brazilian test procedure. In order to avoid the sample to fall apart, sample is wrapped with thin Teflon tape and finally protected by heat shrink Teflon sleeve. After few trial and error, a method was established to induce a single fracture (or as simple as possible) along the cross section of the sample. After inducing the fracture, a new permeability test was conducted, the same way as described above. After this permeability test, the sample was saturated with a 7 wt% sodium silicate solution in a vacuumed chamber. The saturated sample was placed in a cylinder and exposed to CO_2 at 5 bars for approximately 24 hours. And finally, third permeability test was performed on this treated fractured sample.

2.2 MINI-WELLBORE SIMULATOR TESTS

2.2.1 Setup description

Mini-wellbore simulator used in this study was recently developed within the Well Integrity ECCSEL Infrastructure. The Mini-Wellbore simulator is an advanced pressure cell incorporating a downscaled wellbore sample including a casing, cement sheath and surrounding rock, as shown in Figure 6. The outer diameter of the casing is 40 mm. The inner and outer diameter of the core are 2" and 4" inch respectively, and the length is 290 mm. The simulator allows for simultaneous application of pore pressure on the core (up to 200 bar), confining pressure (up to 200 bar) and casing pressure (up to 500 bar). The mini-wellbore simulator is designed for in-situ annular cementing, initiation of fractures, core flooding and injection of remediation fluids. Moreover, the carbon-wrapped core holder (inner diameter or 4") is X-ray transparent and thus allows for in-situ experiments within a CT scanner. Full rotation (360°) is possible while CT scanning. This enables us to observe and follow different processes such as fracture development within cement sheath and rock, or injection of different fluids or sealing materials in real time.

The end caps with the fluid ports are shown in Figure 6 (b), as well as the assembly with steel casing and hollow cylinder rock. The casing is bonded to the rock when cement is injected directly through its own designated ports and hardened under desired pressure.

The ECCSEL mini wellbore simulator is used to investigate field-relevant breach of well integrity; this is achieved by varying the wellbore pressure. Increase and decrease in the wellbore pressure make the steel casing expand and contract, and due to stiffness contrasts with the cement and rock, initiates different types if fractures in those materials. These cycles represent stress changes to be expected during the lifetime of the well, principally due to temperature contrasts for CCS operations upon well shut-in and bean-up. For shale gas operations, pressure variations are obviously related to fracturing stages and later, when in production mode due to rapid depletion and stress shadowing between fractures and their successive closures.

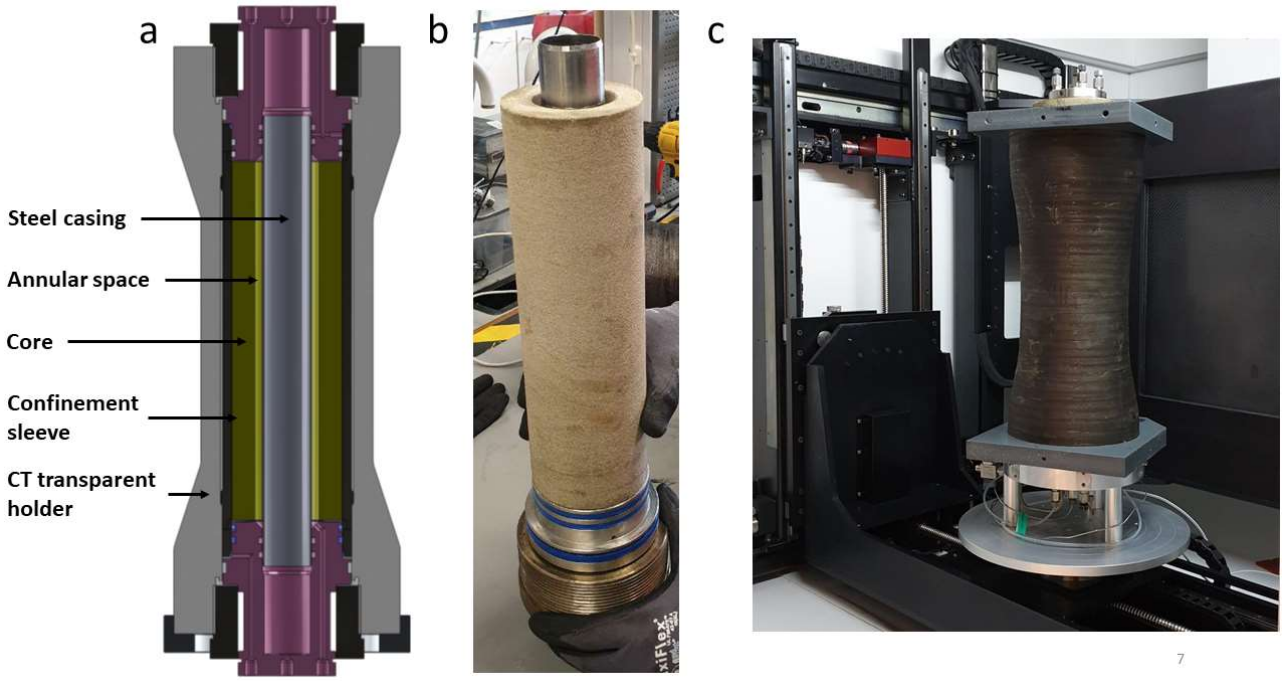

Figure 6 (a) Schematic of the mini-wellbore simulator; (b) Photo of a wellbore sample with the end caps; (c) Mini-wellbore simulator placed in a CT scanner, where CT transparent carbon-wrapped holder is visible.

2.2.2 Wellbore sample preparation and creation of leakage pathways

For pressure cycling experiments in the mini-wellbore simulator we used Castlegate sandstone and Portland G cement. The core holder was assembled and placed vertically, then the core rock saturated with brine for 24 hours. Having a pore fluid is essential to maintain the pore space against collapse when applying

confinement force to the rock. Cement slurry was prepared with a water-to-cement ratio of 0.5. Cement slurry was then injected into the annulus from bottom side of the core holder. The slurry displaces the brine in the annulus, similar as under downhole conditions. We used a peristaltic pump for the injecting purpose. The pump was able to pump the slurry with maximum 10 bar. The pore fluid pressure was maintained with 20 bars for 48 hours until the cement slurry was solid. The same pressure is applied to the confining sleeve. This ensures a uniform high quality of cement in the annulus. The cement was cured at room temperature. An industrial X-ray μ-CT scanner was used for characterization of quality of the cementation and fracturing upon pressure increase and pressure cycling.

The first test was run without confining or pore pressure, and pressure increase was performed inside of the CT scanner, with in-situ CT scanning. The casing pressure was increased stepwise from 50 bars up to 350 bars to induce fractures in the annular cement and rock, as indicated in Table 5. Pressure cycling between 100 and 300 bars was then performed. For the second test, pressure increase and cycling were performed in-situ in the CT scanner with application of confining and pore pressures in addition to the casing pressure. The application of the casing pressure started at 100 bars and went up to 400 bars (Table 5), and CT scanning was repeated after each pressure increase. In the second test, pressure cycling was then performed between 100 and 400 bars. The mini-wellbore simulator was scanned for 360 degrees with different test parameters as shown in Table 5. For both tests, CT scanning was performed with the in-situ pressure conditions. Typical reconstructed CT images (horizontal and vertical cross-sections) of the setup with the wellbore sample are shown in Figure 7.

Table 5 Test parameters: applied confining, pore and casing pressures.

	Confining, P_{sl} [bar]	**Pore, P_p [bar]**	**Casing, P_c [bar]**	**Casing pressure cycling [bar]**
Test 1	0	0	50, 150, 200, 300, 350	100 - 300
Test 2	100	50	0, 100, 250, 300, 350, 400, 450	100 - 400
	85	50	450, 120	N/A

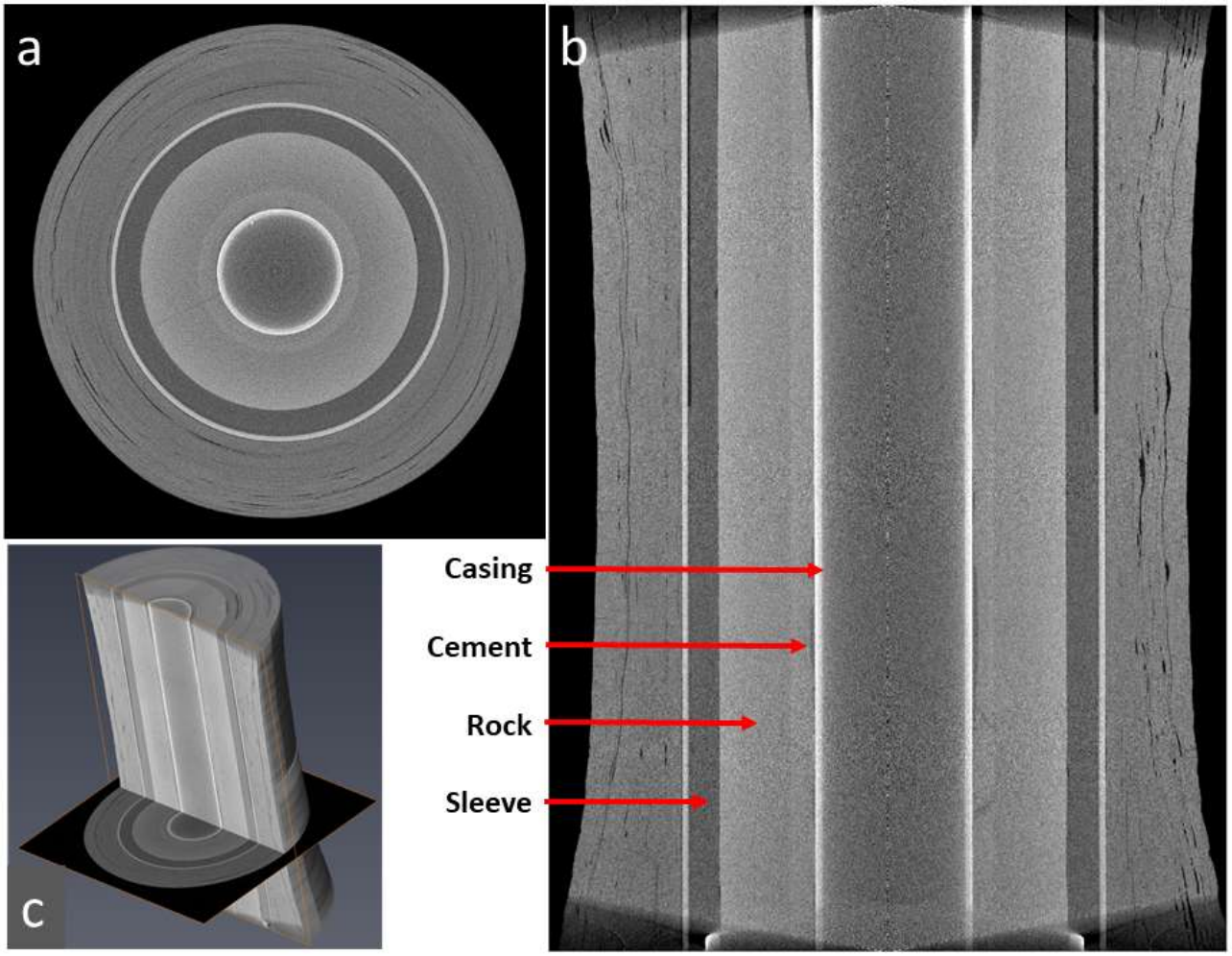

Figure 7 Typical reconstructed CT images of the setup with the sample (from test 1): (a) A horizontal cross section; (b) A central vertical cross section; (c) 3D image rendering of a half of the entire setup exposing the central vertical cross section. Various components of the setup, steel casing, the cement sheet, the rock core, and the sleeve separating the confining pressure from the pore pressure could be distinguished easily.

2.2.3 Sealant injection & permeability measurement

In order to determine the sealing efficiency of the remediation materials, a set of permeability measurements on the min-wellbore simulator was planned after the successful fracturing and X-ray visualization of the in-situ setup. Hence, a baseline (pre-fracture state) permeability measurement was not taken. An overview of the flooding test setup, incorporating the mini-wellbore simulator, is provided in Figure 8. The flooding equipment consists of two high-pressure pumps, one of which is use for brine injection into the rock formation and maintaining the pore pressure (pump-1), and the other for varying the casing pressure (pump-2). The confining pressure is preset and maintained at the same level with a nitrogen-based piston bottle as the pressure regulator. In addition to the pressure readout from the pumps, three independent pressure gauges are mounted on the opposite side for monitoring the pressure variations more precisely. Brine is injected through a high-pressure piston bottle connected to pump-1.

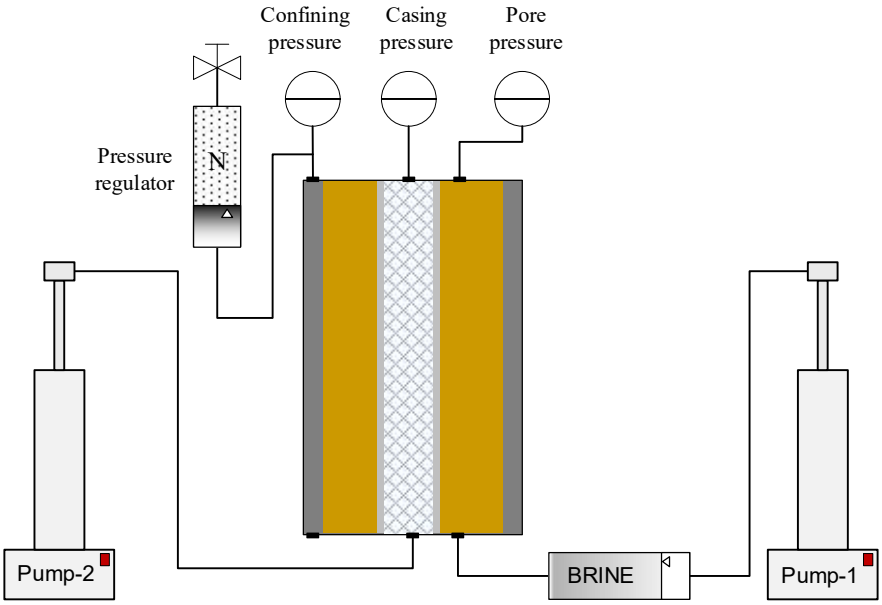

Figure 8 A schematic overview of the flow part of the min-wellbore simulator experimental setup where various components have been exaggerated for illustration purposes. The casing pressure is controlled by pump-2, whereas pump-1 is used to inject the brine into the rock sample for either maintaining the desired pore pressure under integrity tests, or in flooding for permeability measurements.

The measurement data for the permeability tests are given in Table 6.

Table 6. Permeability measurements on mini-wellbore simulator

P_{sleeve}=54 bar	P_{sleeve}=85 bar
Permeability = 151 mD	Permeability = 136 mD

Rate Pump	Q_{meas} [ml/min]	Q_{meas} [ml/s]	ΔP_{54} [mbar]	ΔP_{54} [atm]
0,1	0,094	0,002	15,47	0,015
0,2	0,197	0,003	18,23	0,018
0,3	0,284	0,005	25,65	0,025
0,4	0,387	0,006	33,22	0,032
0,5	0,484	0,008	39,71	0,038
0,6	0,587	0,010	46,23	0,045

Rate Pump	Q_{meas} [ml/min]	Q_{meas} [ml/s]	ΔP_{85} [mbar]	ΔP_{85} [atm]
0,1	0,089	0,001	14,47	0,014
0,2	0,184	0,003	20,80	0,021
0,3	0,281	0,005	28,59	0,028
0,4	0,383	0,006	36,26	0,036
0,5	0,468	0,008	42,63	0,042
0,6	0,586	0,010	49,24	0,049

Using Darcy's law

$$k = \frac{1}{\frac{\Delta P[atm]}{\Delta Q.[\frac{ml}{s}]}} \cdot \frac{L[cm] \cdot \mu[cp]}{A[cm^2]}$$

it is possible to calculate the permeability values as:

- For confining pressure of 54 bar: Permeability = 151 mD
- For confining pressure of 85 bar: Permeability = 136 mD

2.2.4 Data analysis

The CT images were analyzed and segmented into three-dimensional (3D) representations in Avizo Fire software (FEI, Amira & Avizo 3D Software, part of Thermo Fisher Scientific). Sandstone material was defined first and starting from this label other components were distinguished (cement, casing, fractures, void space). Fractures and void spaces were defined by selection of a low intensity range that covered best the void space for the available image resolution. Uncertainty in definition of fractures by this image segmentation method arises from the limited resolution of the CT images, limitations of the image analysis method itself, subjective selection of relevant greyscale ranges, and overlapping intensity for the sandstone matrix, cement and fractures. Although not all fractures, especially the finer ones, could be extracted due to these limitations of the conventional image analysis technique, this method still provided a decent visualization of the more prominent fractures.

3 Results

3.1 PORTLAND G

3.1.1 Preliminary injection tests

UCS tests were conducted on cores constructed of Flexible Portland G and Low-density Portland G to find the strength of the different sealing materials, see Table 7. The experiment was conducted after one week of hardening.

Table 7 Result of Unconfined Compression Test (UCS) on different sealing material.

Sample	Length (mm)	Diameter (mm)	Peak axial stress (MPa)	Young's Modulus (GPa)
Flexible Portland G 1	52.41	25.15	11.18	3.60
Flexible Portland G 2	53.43	25.08	10.88	3.49
Low-density Portland G 1	51.58	25.26	19.13	6.49
Low-density Portland G 2	51.89	25.30	18.84	6.11

The Low-density Portland G had the highest compressive strength and stiffness, approximately twice the magnitude as for the Flexible Portland G. For one of the Flexible Portland G core samples, one large air pocket, approximately 2 mm^2, was observed on the surface. Air pockets of that size could also be present inside both Flexible Portland G samples. This may have affected the strength and stiffness of the cement.

Figure 9 depicts the results obtained from experiments on a prepared slit, described in section 2.1.1. The average pore pressure is plotted as a function of injection rate for the different sealant materials: Low-density Portland G and Flexible Portland G. The reference indicates a sample without any sealant material, hence an open channel. The different Portland G slurries were injected into the open channel and the pore pressure test was conducted after approxemately one month of hardening.

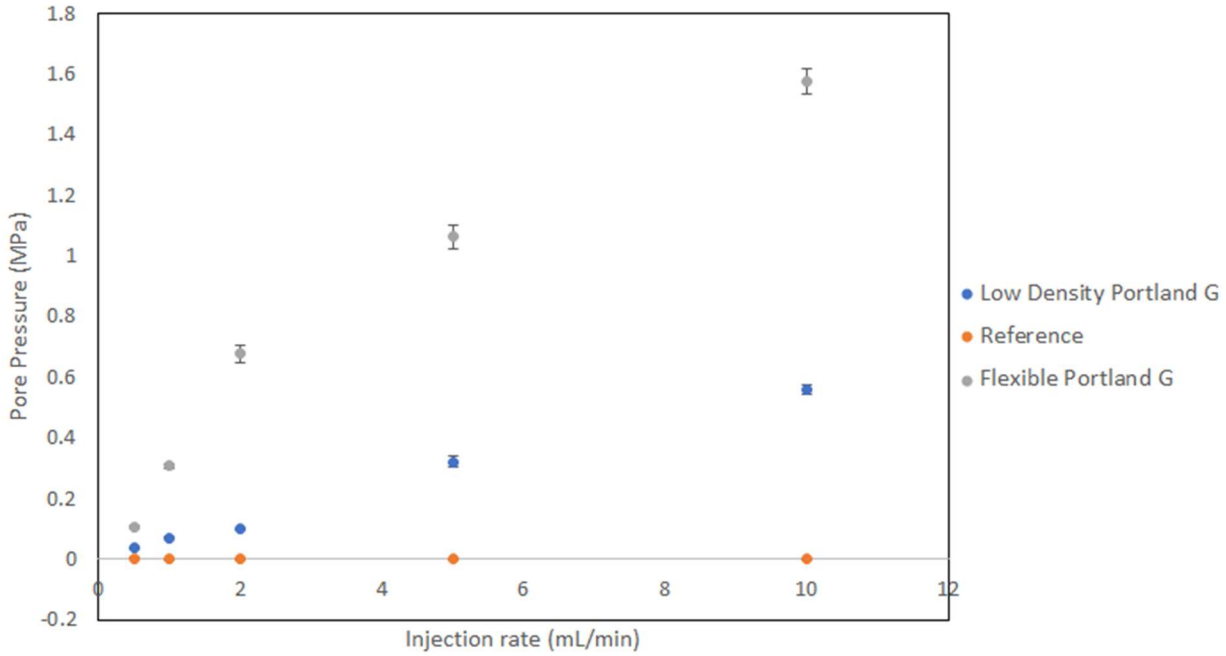

Figure 9 Plot of average pore pressure as a function of injection rate, for Low-density Portland G (blue), Flexible Portland G (grey) and reference (orange).

The plot depicts that the pore pressure increases with increasing injection rate for all samples except the reference, which had a zero-pore pressure build-up. The Flexible Portland G as a sealant material resulted in the highest pore pressure, indicating a good sealing ability. However, after the test there was observed cracks in the top part of the sample, see Figure 10.

Figure 10 Post-test pictures of samples with Low-density Portland G (a) and Flexible Portland G (b) as sealant material.

In Figure 10 it is seen that sample (b), corresponding to the Flexible Portland G, experienced some deformation during the injection of brine. However, this sample obtained the highest pore pressure build-up, meaning the deformation did not affect the sealing ability to that extent that pressure build-up was lost. A reason for this could be that loose cement fragments got pushed further into the sample by the injected brine, hence lowering the permeability. However, the timeline of this experiment was very narrow, and the deformation would probably increase with time, affecting the permeability negatively. µ-CT was conducted to track the deformation within the sample. Cracks and cavities were detected throughout the sealant material, indicating that prolong injection of brine would lead to a higher permeability. µ-CT of the Low-density sample showed cracks and cavities within this sealant material as well, explaining the low pore pressure build-up obtained. Despite the cavities and low pore pressure, Low-density Portland G was chosen as a sealant material to test in the mini-wellbore simulator test. The low viscosity will be beneficial during injection, helping to penetrate as many fractures as possible, without causing too much fracture propagation or creation of new micro-cracks. At the same time, the density of the slurry is close to conventional cement and should therefore guarantee stable displacement of resident brine or gas in the fractures.

3.1.2 Mini-wellbore simulator tests: fracture induction

In the first test in the mini-wellbore simulator, the casing pressure was applied without confining or pore pressure on the rock core. Figure 11 shows CT cross-sectional images after the initial fracturing event and after pressure cycling, at the same position along the cell axis. The CT images revealed that the cement slurry did not fill the annular space completely especially towards the casing (Figure 11) due to poor quality of the cement displacement in the annulus. The void space is visible in Figure 11 (a,b), and it extended almost throughout the entire sample. The opening was larger closer to the top end, which is visible also in Figure 7 (b). However, we decided to continue the planned test since the results would most likely demonstrate a poor cement job scenario. The casing pressure was increased stepwise as explained in Table 5. There were no visible changes in the cement sheath before the internal casing pressure was increased up to 300 bars, when a couple of fractures appeared (Figure 11 (a)). One fracture extended into the rock, while there were a couple of other fractures that appeared only in the cement sheath. The experiment was then continued with pressure cycling between 100 and 300 bars. Figure 11 (b) shows further development of the radial fractures in the annular cement after pressure cycling, and their continuation into the surrounding rock at 300 bars of casing pressure. Pressure cycling induced many new fractures, some of them very fine. Reconstruction of the sample into 3D volume is shown in Figure 12. The radial fractures extended along the sample axis, and this caused the core sample to be split into several pieces while disassembling the setup. No new fractures were observed when pressure was increase beyond 300 bar after the cycling procedure.

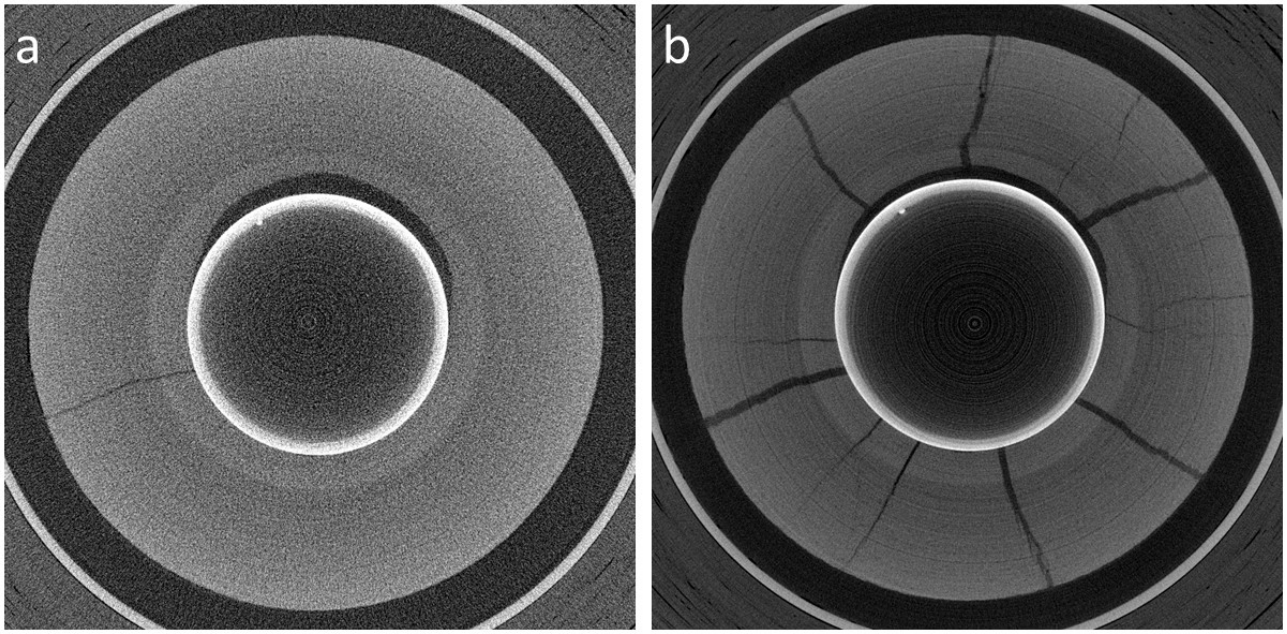

Figure 11 Test 1: Cross-sectional CT images taken at the same position along the cell axis (around sample centre), where opened channel toward the casing is visible: (a) upon the occurrence of the first fractures at 300 bar of casing pressure, and (b) after casing pressure cycling between 100 bar and 300 bar, with CT scanning performed at 300 bar.

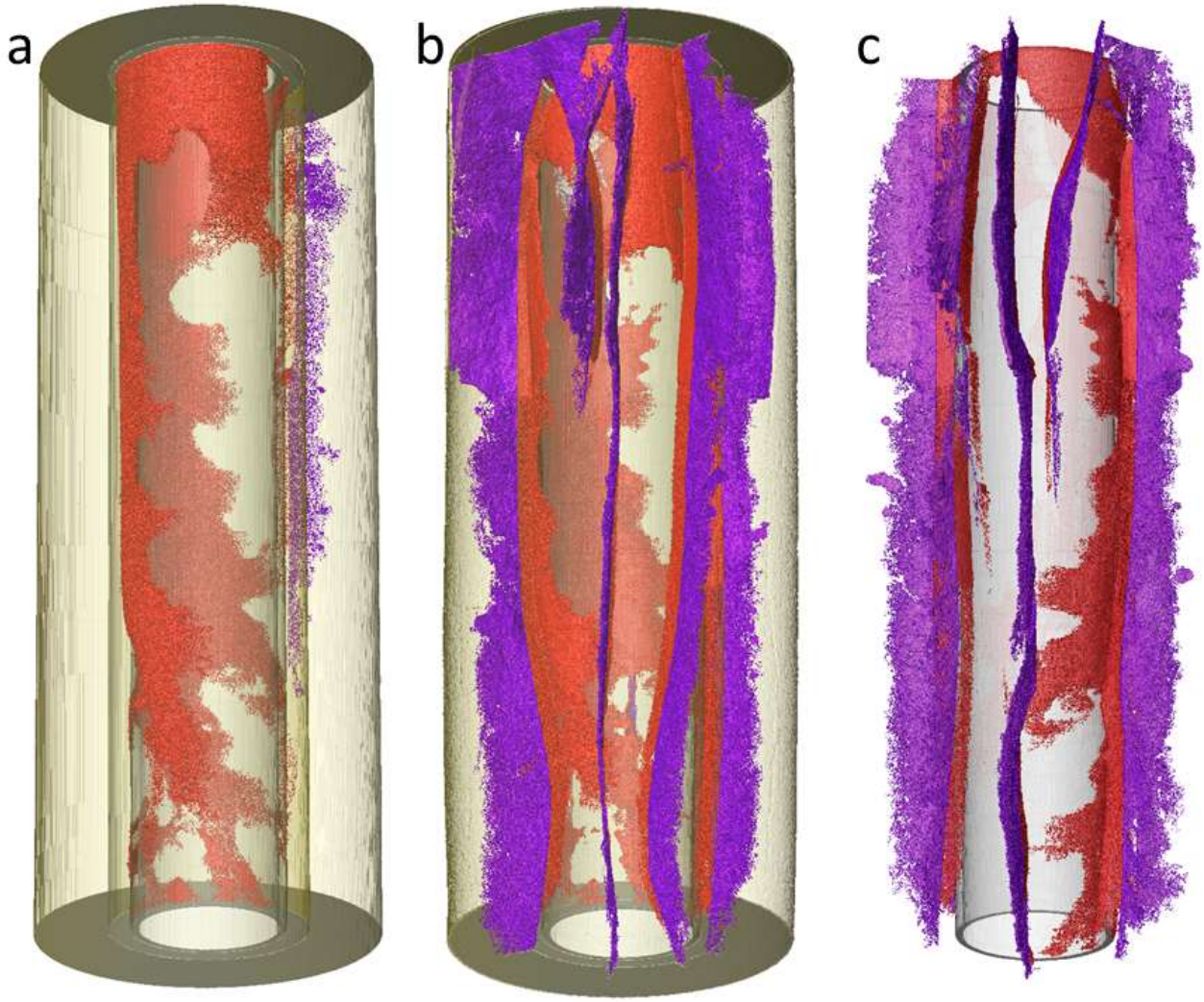

Figure 12 Volume reconstruction of the wellbore sample for test 1: (a) after the initial fracturing; (b) after pressure cycling; (c) after pressure cycling – only casing, fractures and void space shown, in another orientation. Yellow – rock; boundaries between rock and cement and cement and casing are also shown. Red – fractures and void space in the cement sheath; purple – fractures in the rock.

In the second test, the initial conditions of the experimental setup were with application of a confining pressure of 100 bars and a pore pressure of 50 bars. The setup was CT scanned regularly after each step of applied change in the casing pressure, according to Table 5. The casing pressure was increased stepwise up to 400 bar without any fracturing in the cement sheath. Pressure cycling was then conducted between 100 and 400 bar (8 cycles), and still no changes were observed. After the last cycle, the casing pressure was increased to 450 bar. Thus, for confining pressure of 100 bar, no changes in the rock nor the annular cement sheath could be observed for casing pressures up to 450 bar. This may be expected due to the confinement force that was radially applied to the rock in the opposite direction of the casing expansion forces that were imposing a compressive stress in the tangential and radial directions.

Taking into consideration the force balance calculations and the pressure limitations in the setup (450 bars), it was decided to reduce the confining pressure from 100 bars to 85 bars. This resulted in the immediate formation of fractures in both the cement sheet and the surrounding rock. Figure 13 shows the effect of confining pressure reduction from 100 to 85 bars, while the casing pressure and pore pressure were kept constant at 450 bars and 50 bars, respectively. A central vertical CT cross-section and reconstruction of the sample into a 3D volume is shown in Figure 14. The results show that the fractures propagated radially when reducing the confining pressure from 100 to 85 bars. This may be similar to what may happen in the reservoir zone during the reservoir pressure depletion. Permeability measurements at two different confining pressures were performed on the fractured sample. The results are shown in **Error! Reference source not found.**.

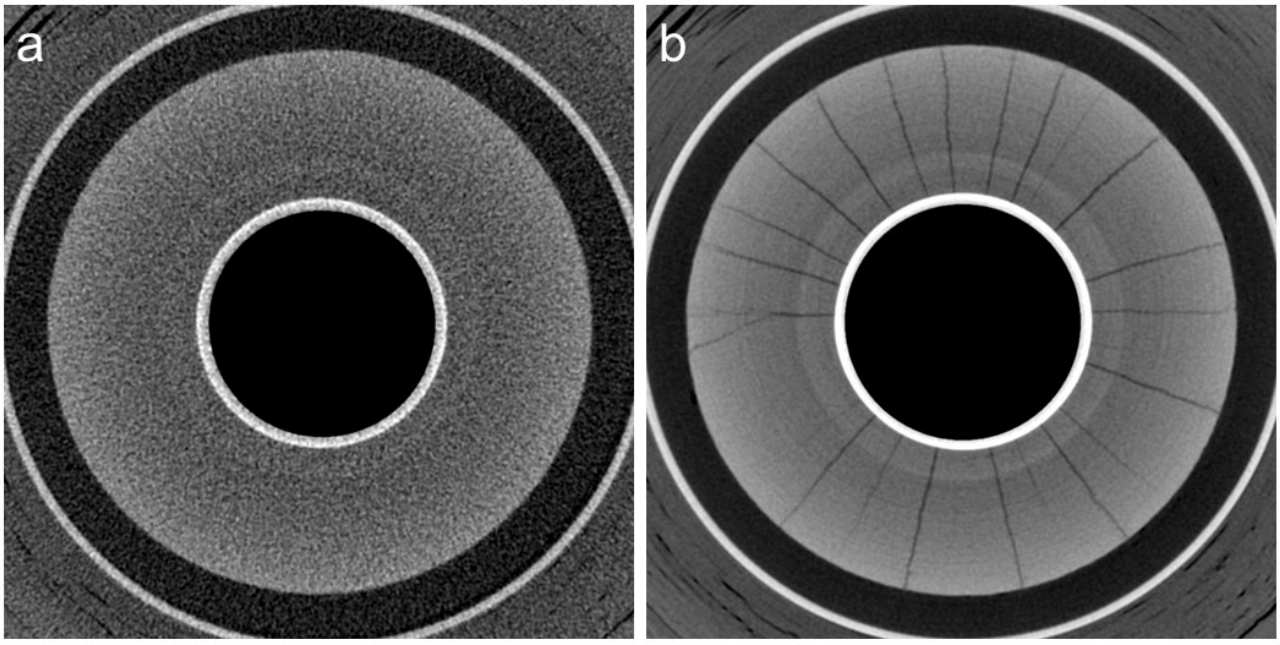

Figure 13 Test 2: Cross-sectional CT images prior to and after the reduction of the confining pressure from (a) 100 bars to (b) 85 bars, at the same position along the cell axis. The casing pressure was kept at 450 bars, while the pore pressure was maintained at 50 bars.

The results from these two experiments show that the fracture patterns in the annular cement sheath and the near wellbore formation are qualitative and quantitively different. This can be corelated with the application of the confining and pore pressures. Applying confining pressure led to a higher fracturing wellbore pressure, a greater number of fractures with both smaller apertures and symmetrical compared to the test with no confinement. This was numerically demonstrated by Gheibi et al. (Gheibi et al., 2019). The fractures that we initiated in these two tests are similar to the observations from previous studies where pressure cycling of the casing was performed (Skorpa et al., 2019; Vrålstad et al., 2019). In these two studies, there was no confining nor por pressure, and only casing pressure was applied stepwise as in the present study. This corresponds to the conditions in the first test. Gradual failure of the cement sheath was observed when it was surrounded by Castlegate sandstone (Skorpa et al., 2019; Vrålstad et al., 2019), from 150 bars to 300 bars when finally, a distinct fracture appeared in the rock as well. This is similar to our observations in the first test, upon the initial fracturing of the cement and rock (Figure 11 (a)).

Another factor that could have affected the pattern and the size of the fractures, to some degree, is the initial quality of the cement sheath. In the first test, a substantial amount of cement was absent, and the casing had a large non-bonded surface. On the other hand, in the second test, the quality of the cementing was much better, and the cement slurry completely filled the annular space. The fracture distribution in the second test was more uniform around the casing. Therefore, the second sample was selected for remediation test as this represented fracture pattern that is expected to occur in the field upon casing pressure variations.

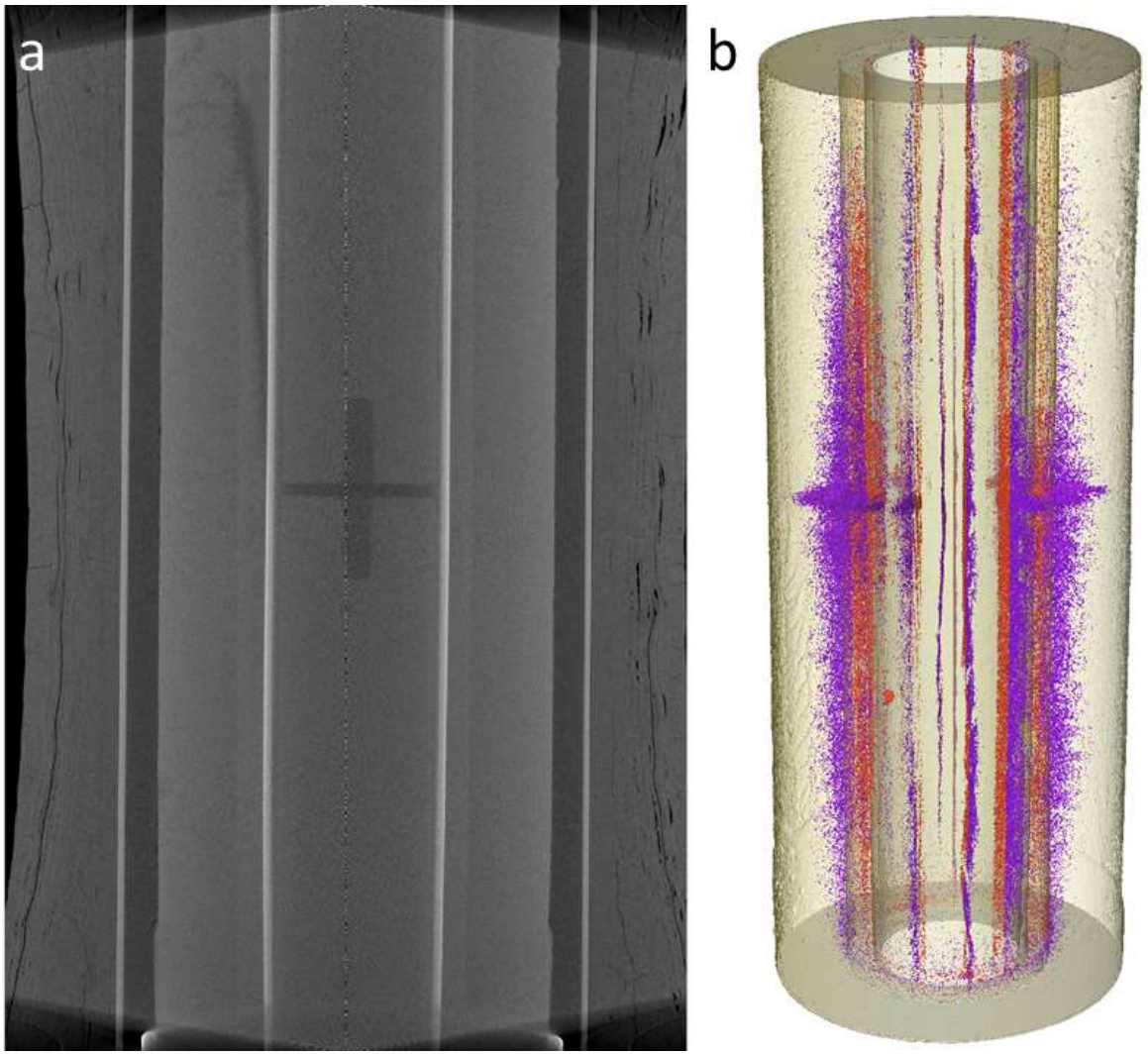

Figure 14 Test 2 after fracturing: (a) a central vertical CT cross-section with one fracture visible; (b) volume reconstruction of the sample. Yellow – rock; boundaries between rock and cement and cement and casing are also shown. Red – fractures and void space in the cement sheath; purple – fractures in the rock.

3.1.3 Mini-wellbore simulator: remediation test

It was not possible to test the silica gel in the mini-wellbore simulator, due to concerns from the above-described tests with this fluid that it may be difficult to make it harden solely inside the intended fracture network and not compromise tubing and connectors which would be difficult to remove. The remediation would also have required accommodating for extra pump and piping for the CO_2 flooding, which was not explored due to low activity in the Covid-19 outbreak period. One remediation test was however carried out, injecting Low-density Portland cement into the fracture network from the second fracturing test described above. This injection was thus made without taking the specimen out of the wellbore simulator, and performed after the permeability test of the fracture pre-remediation.

The sealant was injected into the wellbore simulator through a piston-based transfer vessel, while it was under constant rocking (45 degrees tilt in each direction). The injection process was maintained for ca 30 minutes. The confining pressure was kept at 84 bars and the injection rates increased from 2 ml/min to 8 ml/min. The sealant material could not be detected on the production side of the mini-wellbore simulator. However, a large amount of Portland contaminated brine was produced, indicating that segregation of brine from Portland cement had taken place within either the mii-wellbore simulator or in the piston bottle. No permeability measurement could be made, indicating a possible hardening of the segregated cement between inlet and sandstone core assembly.

Table 8 Permeability after fracturing and after remediation with low-density cement slurry, for test 2.

Test 2	Confining pressure [bar]	Permeability [mD]
After fracturing	54	136
	85	151
After remediation	-	0*
	-	0*

*No flow could be induced, the cement having apparently hardened also between the inlet and the rock core.

3.2 SILICATE GEL

Silica gel was tested as a sealant material by reaction between 7 wt% sodium silicate and gaseous CO_2. The test consisted of experiments on a prepared slit, see section 2.1.2, and an induced fracture on a cement sample, see section 2.1.3.

3.2.1 Preliminary injection tests

Figure 15 depicts the average pore pressure as a function of injection rate for the different pore pressure tests, see section 2.1.2 for experimental description. An increase of pore pressure compared to the reference pressure will indicate a decrease in permeability.

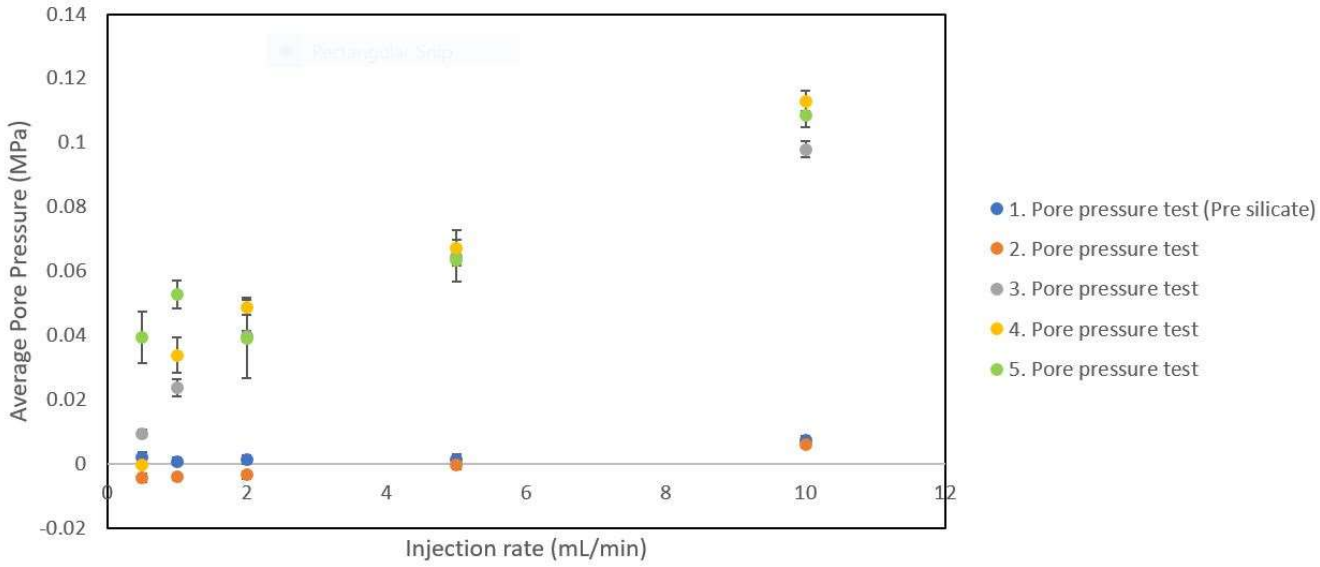

Figure 15 Plot of average pore pressure as a function of injection rate. The different pore pressure tests correspond to what summarized in Table 4.

The blue data points represent the pore pressure prior to adding silica gel. From the plot it is seen that there was no significant difference in the pore pressure after first injection of sodium silicate (orange data points). After the second injection of silicate solution (grey data points), there was a significant increase of pore pressure, increasing with injection rate. A small increase of pore pressure was measured between the third (grey data points) and fourth (yellow data points) test. After the last injection of sodium silicate (green data points), the pore pressure did not increase with injection rate. For injection rate 0.5 and 1 mL/min, the pore pressure was significantly higher compared to previous tests, but the pore pressure decreased when the rate was increased to 2 mL/min. This indicate that some silica gel was lost during this part of the pore pressure test. Since the green data points are not significantly different from the yellow data points (4. Pore pressure test) at rate 2, 5 and 10 mL/min, this suggests that the additional barrier created after the last injection of sodium silicate was lost.

The highest accumulated pore pressure was about 0.12 MPa, which indicate a low sealing effect from the obtained silica gel barrier, especially compared to what obtained for the Portland G sealing materials. The chosen concentration of sodium silicate was selected so that the solution would have a low viscosity. This to prevent clogging of tubing. However, the results of this experiment indicate that the solution used had a too low viscosity to create a sufficient barrier in a channel of this size. When injecting CO_2, a significant portion of the silicate solution migrated to the Castlegate before reacting with CO_2. Hence parts of the increased pore pressure observed was due to the reduction of permeability in the sandstone. However, it was seen that the bottom part of the cement channel contained some solid silica gel. Micro-CT was conducted, and a small silica gel barrier was observed close to the Castlegate interference. This barrier only covered half of the slit area, explaining the low accumulated pore pressure.

Future tests with this concentration of sodium silicate should address more natural fractures. Natural cracks will benefit from low viscosity, as the solution will easily disperse into the fracture network, while at the same

time the fracture network will help maintain the solution to a greater extent than a large channel manages. However, the need for CO_2 to flow evenly and react with the gel remains a disadvantage compared to one-fluid remediation, as proposed with the two cement formulations, unless the leaking CO_2 itself can be used for solidification. This presupposes that the flow rate of leaking gas is adequate to obtain rapid enough strengthening. Future testing in the ECCSEL mini-wellbore simulator thus demands some modifications to the flow lines, in order to guarantee that gelling occurs in the fractures; an envisaged test would be to inject first the silica gel, then shift to dedicated tubing and connectors, dispensing the CO2 gas. This would still only cover the field case where CO2 is not already leaking through the fractures, but is dispensed in a control manner through an opening in the casing below the interval to be treated.

3.2.2 Effect of silica gel treatment on induced fracture permeability

The effect of generating a silica gel barrier using CO_2 under controlled condition on fractured cement was studied by three steps. First (step 1) a permeability test of the initial cement sample was conducted, see

Table 9. Second, a controlled Brazilian test was conducted to create a single (or simple) fracture (step 2), see Figure 17a,b. The sample with the induced fracture underwent a new permeability test, see

Table 9). Last (step 3), the fractured sample was saturated with sodium silicate and placed in a cell where it was exposed to CO_2 gas for a day. This to allow solidification of silica gel see (Figure 17c,d). After solidification, the last permeability test was conducted, see

Table 9. The permeability test timelines are shown in Figure 16.

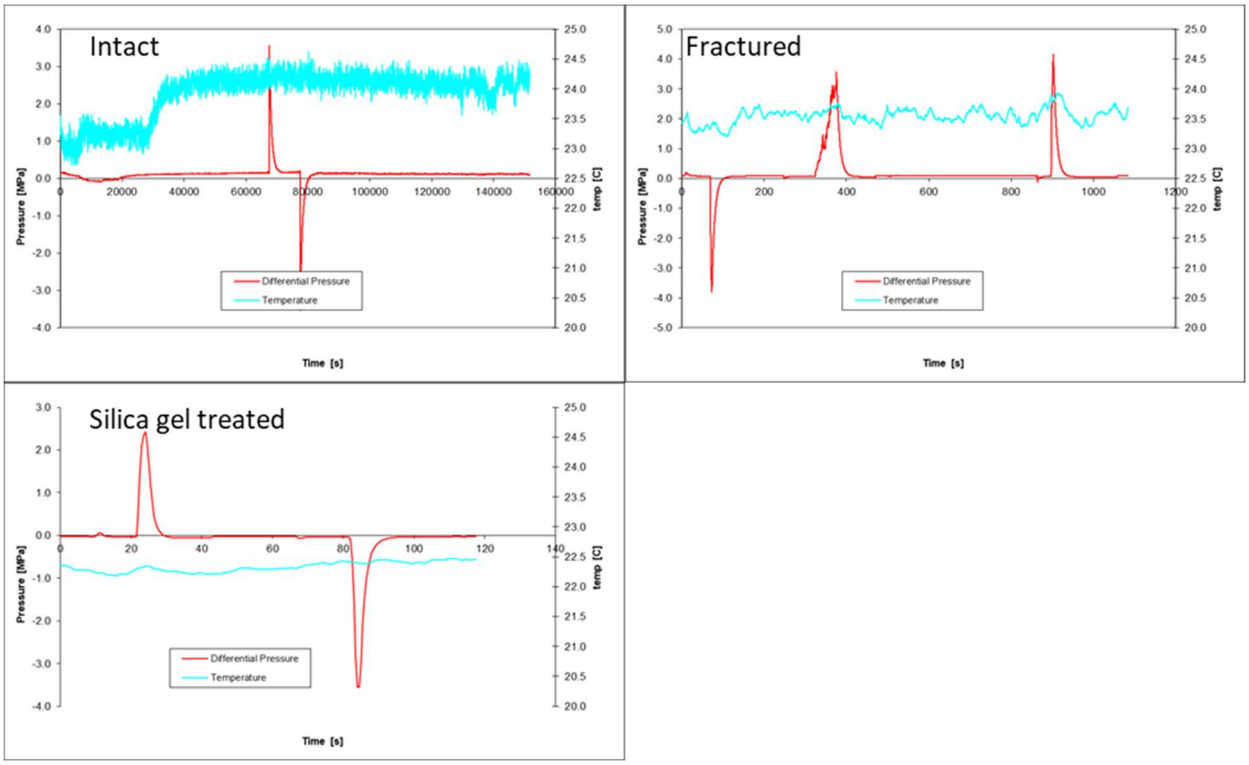

Figure 16 Timeline of permeability tests on cement samples.

Table 9. Data of permeability measured in virgin (initial), fractured and CO_2 treated silica gel in the fracture.

Sample	Permeability [μD]
Initial cement sample	0.81
Fractured cement sample	88.6
Silica gel in fracture	461.2

Data shows that the initial permeability of the cement (virgin sample) is 0.81μD and as anticipated the permeability increased significantly due to presence of fracture(s). The effect of silica gel was not as anticipated. The permeability was drastically higher than its fractured counterpart. After remediation and the last permeability test, the cement sample was taken out of the cell. The sample was intact, and it required force to pull it apart (see Figure 17.

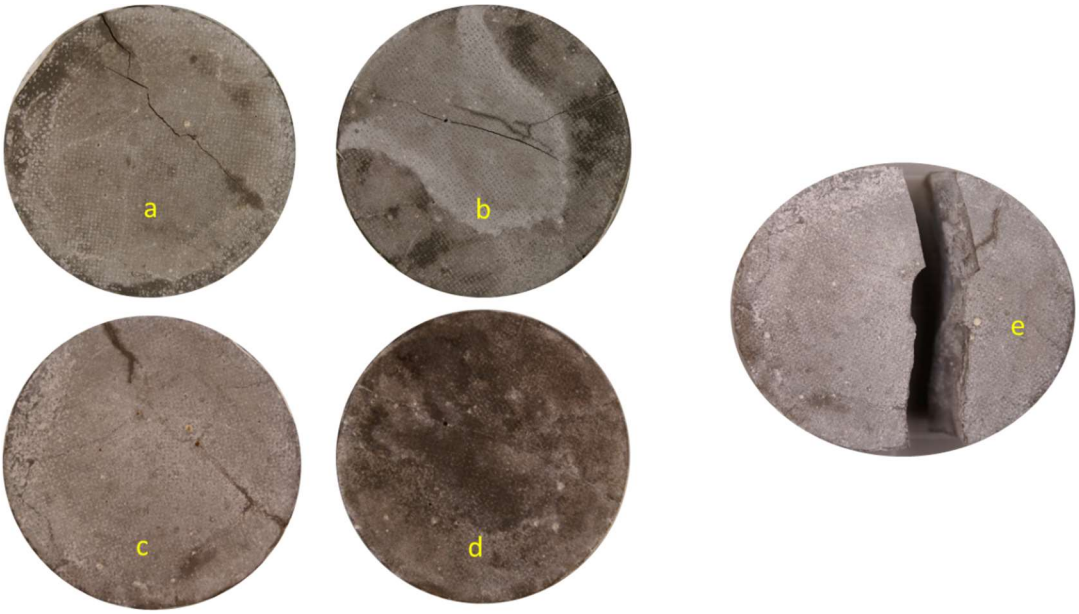

Figure 17. Fractured cement sample after and before silica gel treatment; images 'a' and 'b' indicates the fractured sample before, and images 'c' and 'd' indicate the sample after silica gel treatment. Image 'e' indicate the split sample into two parts along fracture line using hand force.

It was initially thought that silica gel would form a barrier that helped to decrease the permeability, but experimental result showed the completely opposite. Analysing the sample after permeability tests indicate that silica gel has adhesive properties, which keep the sample intact and required force to spit. A possible explanation for the increased permeability could be that CO_2 is not homogenously exposed to the sodium silicate. While the reaction between sodium silicate and CO_2 was ongoing, already solidified, or semi-solidified, silica gel located at the two ends of the fracture could be pushed by the CO_2 gas further into the sample. Since the fracture is not a perfect channel, the preliminary solidified parts could get stuck, and induced the fracture furthermore, see Figure 18.

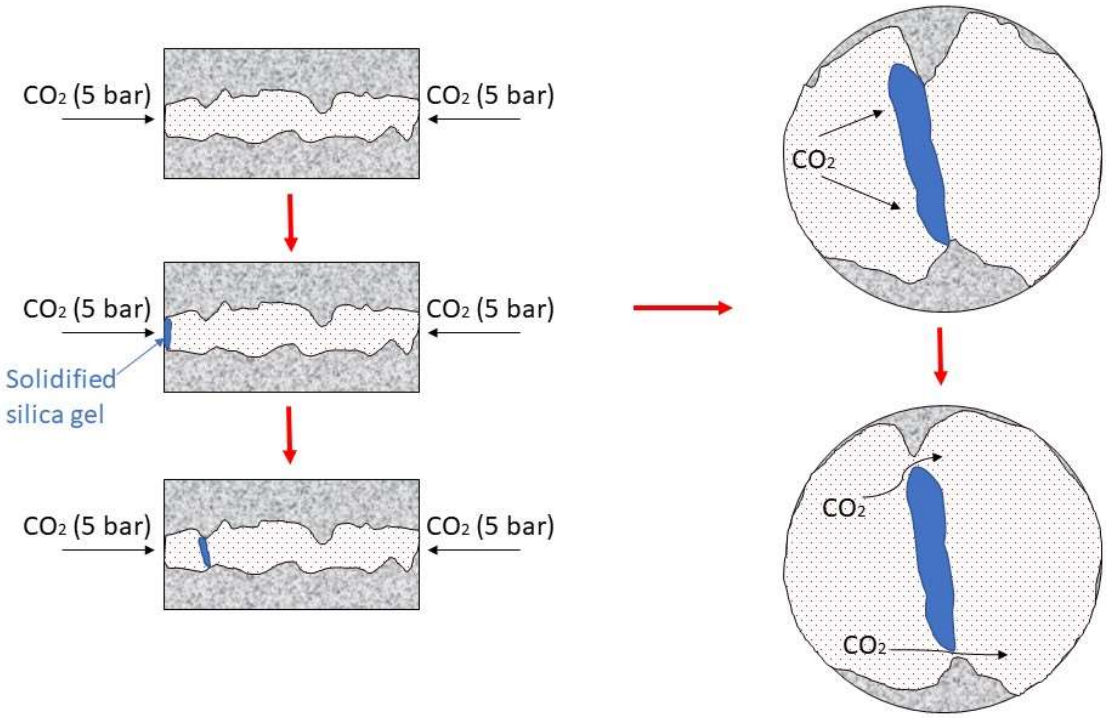

Figure 18 Illustration of the propagation of a solidified, or semi-solidified, silica gel front being pushed into the fracture by the CO_2 gas.

However, this hypothesis is difficult to prove since it is difficult to see any significant change within fracture structure or dimensions from Figure 19.

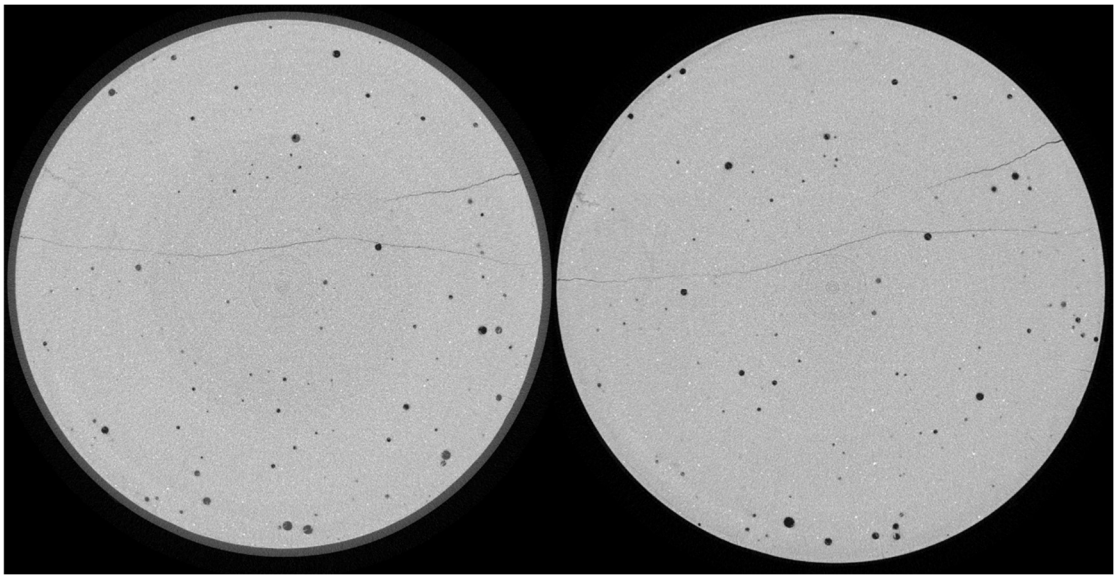

Figure 19. CT scan image of the samples before (left) and after (right) silica gel treatment.

Another probable reason for the increased permeability could be a inhomogeneous distribution of silica gel on the fracture surface, which could create pathways for fluid flow. The sample was subjected to a 15 MPa confining pressure during the permeability test. Since a fractured sample is easier to squeeze compared to a sample with a silica gel filled fracture, fluid flows easier through open fractures during a permeability test.

4 Discussion

This study revealed some interesting results: the method by which the candidate remediation fluids are tested influences the performance of the fluid, which is what is being sought in the first place. The study was incomplete in the sense that not all proposed sealants were tested in all the three experimental setups we used. It is also important to design specific tests for specific problems: is the remediation fluid intended for consolidation and eventual blockage of a permeable formation, thus limiting well fluid leakage away from the well? Or should the fluid remediate fractures already in the cement sheath around the well and discrete fractures extending into the formation beyond? Which type of formation is to be remediated, permeable or impermeable and fractured, such as a caprock shale?

The innovation in this study is two-fold:

- Tailor-made fluids reacting with the leaking fluid at the leakage location in the annulus for remediation of CO_2 wells
- Methodology to evaluate fluid performance in realistic fractures

This study looked at slight modifications to conventional well construction cement to enhance its use as a remediation fluid. Other tailor-made fluids developed elsewhere in WP5 were unfortunately not mature enough to be fairly tested and compared to the fluids tested here, that have been previously used in the field and tested in many laboratory studies. Perhaps most importantly, we believe that the relevance of this study lies in the methodology developed to test candidate fluids against each other in what one could describe as three tiers of complexity. The first tier is the core flooding approach, evaluating performance of the remediation fluid in a well-described slit in an (nearly) impermeable plug. This tier of testing isolates the main feature which is primary performance of the selected fluid inside the created space it needs to repair and eliminates as much as possible interaction with other elements such as type of formation beyond the initial fracture that the treatment is exposed to and the exact topology of the fracture and accompanying network connection to multiple fractures.

The second tier is still focusing on a single fracture, but this time the topology of the fracture is relaxed, therefore more field-realistic. The fracture is stress-induced, opening mainly in tensile mode. The result is a twisting, tortuous flow passage, with aperture depending on the deformation field when applying confining stress and when pressurizing different fluids into it. This added complexity makes analysis of the results more difficult, but at the same time increases field-relevance and highlights potential pitfalls of remediation fluids engineered for simple cases and geometries.

Finally, the third tier is to adopt geometry and complexity comparable to field, but in a scaled down and more controllable setting. This is achieved by the ECCSEL mini-wellbore assembly. Here, radial concentric geometry is introduced, with the correct placement of the different materials, and again with stress-induced fracturing. Now fractures are multiple, connected and traversing either only cement or both cement and surrounding formation. This is the more complex laboratory set-up, making for complicated and long testing campaigns.

This three-tiered approach is very helpful for the industry considering adopting one or the other fluid for its remediation needs. This offers a complete approach, pitching the fluids against each other in different situations. This helps the industry to balance advantages and drawbacks which might be at different tier for the candidate competing fluids. Depending on ease of access for successful placement, type of formation where the leakage occurs, nature of leaking fluid, one might choose one or other fluid as best suited. This will be based on the fluid's performance for each tier of testing proposed here.

This approach obviously also caters for the R&D community, developing new formulations. An obvious starting place is testing under tier one. However, for research into developing a fluid specifically targeting a narrow, specialised application, it may be suitable to jump directly to another tier, or to tailor-make a desired combination of testing materials and conditions. This may involve a particular formation, particular triaxial stress conditions and the presence or flow of specifically determined fluids.

Relevance of the methodology adopted here for other stakeholders is manifested by the fact that the development of remediation fluids is not dissociated from the variety of situations potentially encountered. That is, we try not to only encourage development of chemistries to be tested separately from the whole system that will be encountered in the field. E.g., a particular fluid may be developed to bind to a particular mineral. Success could be demonstrated by studying the reaction itself in an isolated environment. To elicit confidence from as many stakeholders as possible, we proceed to suggest several test environments, highlighting the performance of the proposed solution in different, often worst-case scenarios in terms of implied leakage situation. On the other hand, introducing fluid testing in downscaled field geometry and conditions ensures realistic setting and can sometimes lead to less conservative approaches. The concurrence of geometric effects and downhole stress conditions may entail that a feared leakage situation occurring due to unwanted fracturing, does not lead to immediate escape of fluids to undesired shallower zones; this leads to accrued confidence in our ability to react early and mitigate negative situations without incurring negative consequences.

5 Conclusions

The work performed here has shown that for large fractures in the cement sheath (represented by the rectangular slit experiments in cement plugs), it is difficult to make the silica gel and adhere to the cement walls, if a more permeable formation is found behind it. These tests show that in a realistic situation, where several fluids are present in the system and able to flow, remediation with silica gel is very unlikely. Unless a very complex remediation operation is undertaken where the fractured spot is isolated and washed clear of circulating fluids except the needed CO_2, continuing circulation of resident brine will make permeability mitigation slow and perhaps unsatisfactory. The same silica system performed even worse for a single stress-induced fracture, prepared into a cement plug by subjecting it to a Brazilian tensile test. Here, we were looking again at a situation at depth, so confining pressure was important. The results show that with the reaction between sodium silicate and CO_2 had the unfortunate consequence of increasing the permeability, even above the fractured state that was meant to be mitigated! It is possible that reducing the entry pressure so much that no opening of the fracture and generation of additional microfractures occurred would help reduce the system's permeability, however this again raises complicated operational issues, especially if the CO_2 stream is the leak itself and cannot be easily controlled.

Looking at the available technology of remediation with silica gel, it is apparent that in order to have this flow in the well and penetrate the fractures of interest, it needs to be diluted such that it will not have too high a viscosity and will not solidify on the way to its intended placement. As this solution will react with CO2, it is important to know ahead of treatment where leaking CO2 originates, so as to have the silica gel at the right spot, preferable inside fractures in the cement sheath and not in the well or where it would only partly block the leak.

The silica gel could not be tested in the ECCSEL mini-wellbore simulator, as CO_2 flow capability has not yet been implemented there. However, we can speculate that injecting the solution from below or above, directly in the cement/rock fluid ports (not in the borehole, as it is sealed from the fractures by the steel casing) would have been successful if the fracture network was sufficiently connected or if the surrounding formation was permeable enough. This speculated result is not trivial, since again, fluid compatibility is important for correctly displacing resident brine, pointing to preferring a viscous solution. Good penetration in the fractures prior to gelling points in the other direction, to avoid enlarging the fractures and insufficient coverage. Therefore, the simplest and most effective solution for the fracture network was shown to be low density cement, which was able to penetrate correctly the network and convincingly seal it. Injecting from below in the mini-wellbore simulator can be understood as representing a situation where access has been prepared below the fracture network, by perforating the casing and injecting through this created flow path.

T**he ranking of the tested materials**, based solely on the partial results of this study, is then to prefer regular Portland cement formulations ensuring good flowability and as unobtrusive a penetration of fractures as possible. This could be achieved with the low density and flexible cements. Their advantages were the lack of needed supplementary reaction fluids, ease of preparation and guaranteed density and viscosity advantages for correct brine displacement in the fractures. For large fractures, flexible cement performed better than low-density cement. However, in stress-induced fractures, with more complex topology and tortuosity, the low-density formulation may be preferable. More tests comparing variations on Portland cement formulations are necessary to be able to quantify cost/benefit ratios, taking into account complexity of preparation, curing time, number and cost of desired additives, in addition to flowability and placement ease.

The **guidelines** for remediation treatments are difficult to emit convincingly at this point; we have established several test methodologies that we think satisfactorily represent more diverse and more realistic field situations. Of the fluids tested so far, it would seem that the most sensible approach would be to favour cheaper, more readily available and more widely accepted Portland cement, where the strategy is to have a single slurry, capable of curing already in the cement sheath and in low permeability, fracture formations. More exotic and engineered remediation methods, such as the fluids and materials developed at BGS, University of Nottingham and GEUS, remain to be tested in a similarly varied plethora of rigs; this has not been possible to date, due to the delays brought by the COVID-19 lock-downs and slow start-up of experimental facilities and personnel availability. The same delays occurred at SINTEF, explaining the incomplete tests matrix presented in this report.

Glossary

API American Petroleum Institute.

BFS Blast furnace slag.

BWOC By weight of cement.

CT X-ray computed tomography.

O&G Oil and gas.

6 References

ABDOLLAHI, J, CARLSEN, I M, and WOLLENWEBER, J. 2016. Assessment of Oil & Gas Remediation Technologies for CO_2 Wells. MiReCOL report, D8.3.

ABDULFARRAJ, M, and IMQAM, A. 2020. The potential of using micro-sized crosslinked polymer gel to remediate water leakage in cement sheaths. *Journal of Petroleum Exploration and Production Technology*, Vol.10, 871–881.

AL-ANSARI, A A, AL-REFAI, I M, AL-BESHRI, M H, PINO, R M, LEON, G A, KNUDSEN, K, and SANABRIA, A E. 2015. Thermal Activated Resin to Avoid Pressure Build-up in Casing-Casing Annulus (CCA). Presented at the SPE Offshore Europe Conference and Exhibition, 8th – 11th September, Aberdeen, Scotland, UK. *Society of Petroleum Engineers*, SPE-175425-MS.

API RP 10B-2. 2013. Recommended Practice for Testing Well Cements, Second Edition. *API, Washington, DC*.

AUTEF, A, JOUSSEIN, E, GASGNIER, G, PRONIER, S, SOBRADOS, I, SANZ, J, and ROSSIGNOL, S. 2013. Role of metakaolin dihydroxylation in geopolymer synthesis. *Powder Technology*, Vol. 250, 33–39.

BEHARIE, C, FRANCIS, S, and ØVESTAD, K H. 2015. Resin: An Alternative Barrier Solution Material. Presented at the SPE Bergen One Day Seminar, 22nd April, Bergen, Norway. *Society of Petroleum Engineers*, SPE-173852-MS.

BRYDIE, J R, PERKINS, E H, FISHER, D, GIRARD, M, VALENCIA, M, OLSON, M, and RATTRAY, T. 2014. The Development of a Leak Remediation Technology for Potential Non-Wellbore Related Leaks from CO_2 Storage Sites. *Energy Procedia*, Vol. 63, 4601–4611.

CAO, L, GUO, J, TIAN, J, HU, M, GUO, C, XU, Y, WANG, M, and FAN J. 2018. The ability of sodium metasilicate pentahydrate to adjust the compatibility between synthetic Fluid Loss Additives and Retarders applying in oil well cement. *Construction and Building Materials*, Vol. 158, 835–846.

CARPENTER, R B, GONZALEZ, M E, GRANBERRY, V, and BECKER, T E. 2004. Remediating Sustained Casing Pressure by Forming a Downhole Annular Seal with Low-Melt-Point Eutectic Metal. Presented at the IADC/SPE Drilling Conference, 2nd – 4th March, Dallas, Texas. *Society of Petroleum Engineers*, SPE-87198-MS.

COWAN, K M, HALE, A H, and NAHM, J J. 1992. Conversion of Drilling Fluids to Cements With Blast Furnace Slag: Performance Properties and Applications for Well Cementing. Presented at the SPE Annual Technical Conference and Exhibition, 4th - 7th October, Washington, D.C. *Society of Petroleum Engineers*, SPE-24575-MS.

DAULTON, D J, BOSWORTH, S J, PUMPHREY, B, MCCATHY, S, CANTU, R, and CLENDENNEN, J. 1995. Field Experience With Application of Blast Furnace Slag to the Drilling and Cementing Program in the Stratton Field, South Texas. Presented at the SPE Production Operations Symposium, 2nd - 4th April, Oklahoma City, Oklahoma. *Society of Petroleum Engineers*, SPE-29472-MS.

DAVIDOVITS, J. 2015. *Geopolymer Chemistry & Applications, 4th ed*. (Saint-Quentin, France: Institut Geopolymere.) ISBN 9782951482098

DAVIES, J E. 2017. Using a Resin-Only Solution to Complete a Permanent Abandonment Operation in the Gulf of Mexico. Presented at the SPE Offshore Europe Conference & Exhibition, 5th – 8th September, Aberdeen, United Kingdom. *Society of Petroleum Engineers*, SPE-186113-MS.

DE ANDRADE, J, SANGESLAND, S, SKORPA, R, TODOROVIC, J, and VRÅLSTAD, T. 2016. Experimental Laboratory Setup for Visualization and Quantification of Cement-Sheath Integrity. *SPE Drilling & Completion, Vol.31*, SPE-173871-PA.

DURUCAN, S, KORRE, A, SHI, J -Q, GOVINDAN, R, MOSLEH, M H, and SYED, A. 2016. The use of polymer-gel solutions for CO_2 flow diversion and mobility control within storage sites. *Energy Procedia*, Vol. 86, 450–459.

FLEURY, M, SISSMANN, O, BROSSE, E, and CHARDIN, M. 2016. CO_2 reactive suspensions. MiReCOL report, D9.1.

FLEURY, M, SISSMANN, O, BROSSE, E, and CHARDIN, 2017. A silicate based process for plugging the near well bore formation. *Energy Procedia*, Vol. 114, 4172–4187.

GARBA, M D, 2012. Sodium silicate cement squeeze in massive salt formations: chemistry and chemical evolutions. *Elixir Applied Chemistry*, Vol. 51, 10923–10931.

GHEIBI, S., SANGESLAND, S., and VRÅLSTAD, T. 2019. Numerical Modeling of Radial Fracturing of Cement Sheath Caused By Pressure. Proceeding of ASME 2019 38th International Conference on Ocean, Offshore and Arctic Engineering (OMAE2019). Volume 8: Polar and Arctic Sciences and Technology; Petroleum Technology. OMAE2019-96319.

HO, J F, TAVASSOLI, S, PATTERSON, J W, SHAFIEI, M, HUH, C, BOMMER, P M, BRYANT, S L, and BALHOFF, M T. 2016. The Use of a pH-Triggered polymer gelant to seal cement fractures in Wells. *SPE Drilling & Completion*, Vol. 31, 225–235, SPE-174940-PA.

HOULSBY, A C.1990. *Construction and design of cement grouting, 1st edition.* (New York: John Wiley & sons Inc.) ISBN 13 978 0471516293

KHANNA, M, SARMA, P, CHANDAK, K, AGARWAL, A, and KUMAR, A. 2018. Unlocking the Economic Potential of a Mature Field Through Rigless Remediation of Microchannels in a Cement Packer Using Epoxy Resin and Ultrafine Cement Technology to Access New Oil Reserves. Presented at the SPE/IADC Middle East Drilling Technology Conference and Exhibition, 29th - 31st January, Abu Dhabi, UAE. *Society of Petroleum Engineers*, SPE-189350-MS.

KARAS, D, DEMIĆ, I, KULTYSHEVA, K, ANTROPOV, A, BLAGOJEVIĆ, M, NEELE, F, PLUYMAEKERS, M, and ORLIĆ, B. 2016. First field example of remediation of unwanted migration from a natural CO_2 reservoir: the Bečej field, Serbia. *Energy Procedia*, Vol. 86, 69–78.

KHALIFEH, M, SAASEN, A, VRÅLSTAD, T, BØVIK LARSEN, H, and HODNE, H. 2016. Experimental study on the synthesis and characterization of aplite rock-based geopolymers. *Journal of Sustainable Cement-Based Materials*, Vol. 5, 233–246.

KHALIFEH, M, TODOROVIC, J, VRÅLSTAD, T, SAASEN, A, and HODNE, H. 2017. Long-term durability of rock-based geopolymers aged at downhole conditions for oil well cementing operations. *Journal of Sustainable Cement-Based Materials*, Vol. 6, 217–230.

KHALIFEH, M, SAASEN, A, HODNE, H, GODØY, R, and VRÅLSTAD, T. 2018. Geopolymers as an Alternative for Oil Well Cementing Applications: A Review of Advantages and Concerns. *Journal of Energy Resources Technology*, Vol. 140, 092801.

KORRE, A, GOVINDAN, R, MOSLEH, M H, DURUCAN, S, HEINEMANN, N, and WILKINSON, M. 2017. Report on individual remediation techniques scoring method and classification/ranking results. MiReCOL report, D11.2.

KNUDSEN, K, LEON, G A, SANABRIA, A E, ANSARI, A, and PINO, R M. 2014. First Application of Thermal Activated Resin as Unconventional LCM in the Middle East. Presented at the International Petroleum Technology Conference, 10th – 12th December, Kuala Lumpur, Malaysia. *International Petroleum Technology Conference*, IPTC-18151-MS.

LAKATOS, I, MEDIC, B, JOVICIC, D, BASIC, I, and LAKATOS-SZABO, J. 2009. Prevention of Vertical Gas Flow in a Collapsed Well Using Silicate/Polymer/Urea Method. Presented at the SPE International Symposium on Oilfield Chemistry, 20th – 22nd April, The Woodlands, Texas. *Society of Petroleum Engineers*, SPE-121045-MS.

LAKATOS, I, and LAKATOS-SZABO, J. 2012a. Reservoir Conformance Control in Oilfields Using of Silicates: State-of-the-Arts and Perspectives. Presented at the SPE Annual Technical Conference and Exhibition, 8th – 10th October, San Antonio, Texas. *Society of Petroleum Engineers*, SPE-159640-MS.

LAKATOS, I, LAKATOS-SZABO, J, SZENTES, G, and VAGO, A. 2012b. Improvement of silicate well treatment methods by nanoparticle fillers. Presented at the SPE International Oilfield Nanotechnology Conference and Exhibition, 12th – 14th June, Noordwijk, The Netherlands. *Society of Petroleum Engineers*, SPE-155550-MS.

LAKATOS, I, SZENTES, G, TORO, M, KARAFFA, Z, and VAGO, A. 2020. Mitigation of Formation Damage Caused by Chemical Overdosing in Water Shut-Off Treatments. Presented at the SPE International Conference and Exhibition on Formation Damage Control, 19th – 21st February, Lafayette, Louisiana, USA. *Society of Petroleum Engineers*, SPE-199292-MS.

LI, D, Zhang, L, REN, B, and REN, S. 2014. Experimental Study of CO_2-Sensitive Chemicals for Enhanced Sealing of Leakage Pathways in CO_2 Geological Storage Process. *Energy Procedia*, Vol. 63, 4646–4657.

MANCEAU, J -C, HATZIGNATIOU, D G, DE LARY, L, JENSEN, N B, and REVEILLERE, A. 2014. Mitigation and remediation technologies and practices in case of undesired migration of CO_2 from a geological storage unit – Current status. *International Journal of Greenhouse Gas Control*, Vol. 22, 272–290.

MOSLEH, M H, GOVINDAN, R, SHI, J -Q, DURUCAN, S, and KORRE, A. 2016. Application of Polymer-Gel Solutions in Remediating Leakage in CO_2 Storage Reservoirs. *Society of Petroleum Engineers*, SPE-180135-MS.

MOSLEH, M H, DURUCAN, S, SYED, A, SHI, J -Q, KORRE, A, and NASH, G. 2017. Development and characterisation of a smart cement for CO_2 leakage remediation at wellbores. *Energy Procedia*, Vol. 114, 4147–4153.

NELSON, E B, and GUILLOT, D. 2006. *Well Cementing, 2nd edition.* (Sugar Land, Texas: Schlumberger.) ISBN 13 978 0978853006

ÖZODABAŞ, A, and YILMAZ, K. 2013. Improvement of the performance of alkali activated blast furnace slag mortars with very finely ground pumice. *Contruction and Building Materials*, Vol. 48, 26–34.

PIKE, W J. 1997. Cementing multilateral wells with latex cement. *Journal of Petroleum Technology*, Vol. 49, SPE-0897-0849-JPT.

SAASEN, A, SALMELID, B, BLOMBERG, N, YOUNG, S P, and JUSTNES, H. 1994. The Use of Blast Furnace Slag in North Sea Cementing Applications. Presented at the European Petroleum Conference, 25th – 27th October, London, United Kingdom. *Society of Petroleum Engineers*, SPE-28821-MS.

SALEHI, S, KHATTAK, M J, ALI, N, and RIZVI, H R. 2016. Development of Geopolymer-based Cement Slurries with Enhanced Thickening Time, Compressive and Shear Bond Strength and Durability. Presented at the IADC/SPE Drilling Conference and Exhibition, 1st – 3rd March, Fort Worth, Texas, USA. *Society of Petroleum Engineers*, IADC/SPE-178793-MS.

SANABRIA, A E, KNUDSEN, K, and LEON, G A. 2016. Thermal Activated Resin to Repair Casing Leaks in the Middle East. Presented at Abu Dhabi International Petroleum Exhibition & Conference, 7th – 10th November, Abu Dhabi, UAE. *Society of Petroleum Engineers*, SPE-182978-MS.

SKORPA, R, WERNER, B, and VRÅLSTAD, T. 2019. Effect of rock on cement sheath integrity: shale vs. sandstone. Presented at the ASME 2019 38th International Conference on Ocean, Offshore and Arctic Engineering (OMAE2019), 9th – 14th June, Glasgow, Scotland. OMAE2019-96738.

SUKMAK, P, HORPIBULSUK, S, SHEN, S L, CHINDAPRASIRT, P, and SUKSIRIPATTANAPONG, C. 2013. Factors influencing strength development in clay – fly ash geopolymer. *Construction and Building Materials*, Vol. 47, 1125–1136.

SUN, F, LV, G, and JIN, J. 2006. Application and research of latex tenacity cement slurry system. Presented at the International Oil & Gas Conference and Exhibition in China, 5th – 7th December, Beijing, China. *Society of Petroleum Engineers*, SPE-104434-MS.

SYED, A, PANTIN, B, DURUCAN, S, KORRE, A, and SHI, J -Q. 2014. The use of polymer-gel solutions for remediation of potential CO_2 leakage from storage reservoirs. *Energy Procedia*, Vol. 63, 4638–4645.

TAVASSOLI, S, HO, J F, SHAFIEI, M, HUH, C, BOMMER, P, BRYANT, S, and BALHOFF, M T. 2018. An experimental and numerical study of wellbore leakage mitigation using pH-triggered polymer gelant. *Fuel*, Vol. 217, 444–457.

TAVASSOLI, S, SHAFIEI, M, MINNIG, C, GISIGER, J, RÖSLI, U, PATTERSON, J, THEURILLAT, T, MEJIA, L, GOODMAN, H, ESPIE, T, and BALHOFF, M. 2019. Pilot Case Study of Wellbore Leakage Mitigation using pH-Triggered Polymer Gelant. Presented at the SPE/ICoTA Well Intervention Conference and Exhibition, 26th – 27th March, The Woodlands, Texas, USA. *Society of Petroleum Engineers*, SPE-194251-MS.

TONGWA, P, NYGAARD, R, BLUE, A, and BAI, B. 2013. Evaluation of potential fracture-sealing materials for remediating CO_2 leakage pathways during CO_2 sequestration. *International Journal of Greenhouse Gas Control*, Vol. 18, 128–138.

TODOROVIC, J, VRÅLSTAD, T, BUDDENSIEK, M, and WOLLENWEBER, J. 2016a. Overview of available well leakage remediation technologies and methods in oil and gas industry. MiReCOL report, D8.2.

TODOROVIC, J, RAPHAUG, M, LINDEBERG, E, VRÅLSTAD, T, and BUDDENSIEK, M L. 2016b. Remediation of Leakage through Annular Cement Using a Polymer Resin: A Laboratory Study. *Energy Procedia*, Vol. 86, 442-449.

VRÅLSTAD, T, TODOROVIC, J, WOLLENWEBER, J, ABDOLLAHI, J, KARAS, D, and BUDDENSIEK, M. 2015. Description of leakage scenarios for consideration in the work in SP3. MiReCOL report, D8.1.

VRÅLSTAD, T, SKORPA, R, and WERNER, B. 2019. Experimental Studies on Cement Sheath Integrity During Pressure Cycling. Presented at the SPE/IADC Drilling International Conference and Exhibition, 5th – 7th March, The Hague, Netherlands. *Society of Petroleum Engineers*, SPE/IADC-194171-MS.

WESSEL-BERG, D, MOSLEH, M H, GOVINDAN, R, SHI, J -Q, KORRE, A, DURUCAN, S, and DRYSDALE, R. 2015. Gel and foam injection as flow diversion option in CO_2 storage operations. MiReCOL report, D3.3.

WIESE, B U, FLEURY, M, BASIC, I, ABDOLLAHI, J, PATRNOGIC, A, HOFSTEE, C, CARLSEN, I M, WOLLENWEBER, J, SCHIMDT-HATTENBERGER, C, DRYSDALE, R, and KARAS, D. 2019. Near well-bore sealing in the Bečej CO_2 reservoir: Field tests of a silicate based sealant. *International Journal of Greenhouse Gas Control*, Vol. 83, 156–165.

ZUHUA, Z, XIAO, Y, HUAJUN, Z, and YUE, C. 2009. Role of water in the synthesis of calcined kaolin-based geopolymer. *Applied Clay Science,* Vol. 43, 218–223.